Restoration of Foxp3$^+$ regulatory T cells by HDAC-dependent epigenetic modulation plays a pivotal role in resolving pulmonary arterial hypertension pathology

Chien-Nien Chen[1], Nabil Hajji[1], Fu-Chiang Yeh[1,4], Sunniyat Rahman[1,5], Souad Ali,[1] John Wharton[1], Nicoleta Baxan[1], Lin Zhao[1], Chong-Yang Xie[1], Yi-Guan Chen[1], Maria G. Frid[2], Prakash Chelladurai[3], Soni Savai Pullamsetti[3,6], Kurt R. Stenmark [2], Martin R. Wilkins[1] and Lan Zhao[1*].

[1] National Heart and Lung Institute, Faculty of Medicine, Imperial College London, Hammersmith Hospital, Du Cane Road, London, UK

[2] Department of Pediatrics and Medicine, Division of Critical Care Medicine and Cardiovascular Pulmonary Research Laboratories, University of Colorado Denver, Denver, CO, United States

[3] Max-Planck Institute for Heart and Lung Research, Member of German Center for Lung Research, Giessen, Germany

[4] Division of Rheumatology, Immunology and Allergy, Department of Medicine, Tri-Service General Hospital, National Defense Medical Center, Taipei, Taiwan

[5] Department of Haematology, University College London Cancer Institute, University College London, London, UK

[6] Institute of Molecular Biology and Tumor Research, Marburg, Germany

Correspondence and requests for reprints should be addressed to Lan Zhao, M.D., Ph.D., Imperial College London, National Heart and Lung Institute, Hammersmith Campus, Du Cane Road, London, W12 0NN, UK. E-mail: l.zhao@imperial.ac.uk

(This article has an online data supplement, which is accessible from this issue's table of content online at www.atsjournals.org)

Abstract

Rationale: Immune dysregulation is a common feature of pulmonary arterial hypertension (PAH). Histone deacetylase (HDAC)-dependent transcriptional reprogramming epigenetically modulates immune homeostasis and is a novel disease-oriented approach in modern times.

Objectives: To identify a novel functional link between HDAC and regulatory T cells (Tregs) in PAH, aiming to establish disease-modified biomarkers and therapeutic targets.

Methods: Peripheral blood mononuclear cells (PBMCs) were isolated from idiopathic PAH (IPAH) patients and rodent models of pulmonary hypertension (PH): monocrotaline (MCT), Sugen5416-hypoxia (SuHx) rats and Treg-depleted mice. HDAC inhibitor Vorinostat (SAHA) was used to examine the immune modulatory effects *in vivo*, *ex vivo* and *in vitro*.

Measurements and Main Results: Increased HDAC expression was associated with reduced $Foxp3^+$ Tregs and increased programmed cell death-1 (PD-1) signalling in PBMCs from IPAH patients. SAHA differentially modified a cluster of epigenetic-sensitive genes and induced $Foxp3^+$ Treg conversion in IPAH T cells. Rodent models recapitulated these epigenetic aberrations and T cell dysfunction. SAHA attenuated PH phenotypes and restored FOXP3 transcription and Tregs in PH rats; interestingly, the effects were more profound in female rats. Selective depletion of $CD25^+$ Tregs in SuHx mice neutralized the effects of SAHA.

Furthermore, SAHA inhibited endothelial cytokine/chemokine release upon stimulation and subsequent immune chemotaxis.

Conclusions: Our results indicated HDAC aberration was associated with Foxp3^{+} Treg deficiency and demonstrated an epigenetic-mediated mechanism underlying immune dysfunction in PAH. Restoration of Foxp3^{+} Tregs by HDACi is a promising approach to resolve PH pathology, highlighting the potential benefit of developing “epigenetic therapies” for PAH.

Scientific Knowledge on the Subject

Immune dysregulation underlies pulmonary arterial hypertension (PAH) pathogenesis. The impairment of Foxp3$^+$ regulatory T cells (Tregs) perturbs immune homeostasis and is strongly correlated with the prognosis of PAH patients.

What This Study Adds to the Field

In this study, we identified a novel functional link between aberrant histone deacetylase (HDAC) activity and Foxp3$^+$ Treg deficiency in idiopathic PAH (IPAH) patients and pulmonary hypertension animals. In parallel increased PD-1$^+$ T cells were an 'exhaustion' marker signifying pro-inflammatory T cell over-activation. T cells from idiopathic PAH patients exhibited a cluster of epigenetic-sensitive genes involved in the immune-vascular interactions, presenting higher susceptibility to HDAC inhibition. Restoration of Foxp3$^+$ regulatory T cells by HDAC inhibition is a novel disease-oriented approach targeting PAH immunopathy.

Pulmonary arterial hypertension (PAH) pathology is a life-threatening disease. The underlying vascular pathology is complex, characterized by excessive proliferation and inflammation (1), challenging currently available treatments. Accumulating evidence supports a significant role of immune dysregulation in the pathogenesis of PAH (2, 3). Aberrant numbers and dysfunction of $CD4^+CD25^+Foxp3^+$ regulatory T cells (Tregs), a typical immunopathy of autoimmunity, have been reported in various forms of PAH in human and rodent models and associated with disease susceptibility and progression (4–9). Tregs are potent self-tolerance modulators in immune homeostasis, affecting lineage commitment/differentiation/activation of other lymphocyte subsets and suppressing pro-inflammatory responses (10).

The dynamics of circulating immune cells are regulated and fine-tuned by epigenetic mechanisms, such as histone acetylation (11). Histone deacetylases (HDACs) control chromatin accessibility and therefore transcriptional activity; aberrant expression of HDACs is a common feature of autoimmune diseases, inflammatory diseases (12) and cancers, correlating with clinical prognosis (13). Our group previously reported increased expression of HDAC1 and 5 in remodeled vessels in human idiopathic PAH (IPAH) lungs and that HDAC inhibitors (HDACi), namely, SAHA (suberoylanilide hydroxamic acid, Vorinostat) and valproic acid (VPA), reversed hypoxia-induced pulmonary hypertension (PH) in rats via anti-proliferative and anti-inflammatory effects (14). HDACi have been shown to arrest neoplastic cell growth (13) as well as modulate the activation and plasticity of immune cells, especially T cells (15).

Several HDACi, including SAHA, are approved treatments for human T cell malignancy and are under clinical evaluation for other cancers. HDACi enhance Treg function by constitutive Foxp3 activation, promoting thymic production of Tregs and peripheral conversion of T cells into Tregs (15).

In the present study, we sought to explore the role of histone acetylation in PH immune responses, by a) characterizing lymphocyte subtype composition, especially the T cell subset, Tregs, as well as HDAC expression patterns in peripheral mononuclear cells (PBMCs) from IPAH patients and rodent PH models; b) identifying the specific responses to epigenetic intervention by using SAHA and potential epigenetic-sensitive gene clusters in IPAH T cells; c) exploring the immune modulatory effects of HDAC inhibitors SAHA and VPA *in vivo* in monocrotaline (MCT) rats, sugen hypoxia (SuHx) rats and mice (Treg-depleted), and *in vitro* in human pulmonary artery endothelial cell (HPAECs) culture. We propose a novel therapeutic strategy to target PAH immunopathy by epigenetic modulation.

METHODS

All materials, datasets, and protocols used in this study are available to investigators upon request for reproducing the results or replicating the procedure. The full experimental details, including PBMC isolation, human pulmonary artery endothelial cell (HPAEC) experiments, fluorescence-activated cell sorting (FACS) analysis, protein/mRNA expression,

transcriptome analysis with RNA sequencing, chromatin immunoprecipitation (ChIP), as well as *in vivo* hemodynamic and histological measurements, are described in the online supplement.

Human samples

Human samples from 41 IPAH patients and 37 healthy volunteers (Table 1) were obtained after the subjects provided informed written consent, as approved by the local Research Ethics Committee 11/LO/0395. IPAH was diagnosed according to international guidelines (16) by expert physicians at the pulmonary hypertension clinic. The ancestry composition of IPAH patients in this cohort is white British/Asian/other = 31/4/6. Healthy volunteers without cardiovascular, respiratory, and hematologic diseases based on records held by their family practitioners were recruited over the same period as IPAH patients at the clinical research facility in Hammersmith Hospital.

Human ex vivo Treg conversion with HDAC inhibitors

$CD4^+CD25^-$ T cells (Treg-depleted) were purified from PBMCs (9 IPAH patients and 7 healthy volunteers) using magnetic-activated cell sorting (MACS) with CD4 and CD25 isolation kit (Miltenyi Biotec) and we conducted the *ex vivo* experiment with/without the pan-

HDAC inhibitor SAHA treatment (500 nM for 6 days) (17), followed by FACS analysis, RT-qPCR and RNA sequencing. Pathway enrichment analysis of differentially expressed genes from RNA sequencing was performed using GAGE (generally applicable gene-set enrichment) R package (version 2.34.0) with KEGG (Kyoto Encyclopedia of Genes and Genomes) and GO (Gene Ontology) databases; functional assessment using GO (gene ontology) enrichment analysis/PANTHER Classification System; protein-protein interactions and network analysis using Reactome pathway analysis/NetworkAnalyst (networkanalyst.ca) (details in the online supplement).

PH rodent models

All animal experiments were conducted in accordance with scientific procedures approved by the UK Home Office under Animals Act 1986. The protocols are also approved and reviewed by Imperial College Animal Welfare and Ethical Review Body.

Three PH models (details in the online supplement) were used: monocrotaline (MCT) rats, Sugen5416-hypoxia (SuHx) rats and mice (Treg-depleted). Adult age-matched rats/mice were randomly allocated to groups, and all personnel involved in data collection and analysis were blinded to the treatment status of the animals. The sample sizes were selected based on previous literature (18) and listed in each figure legend.

Statistics

All data are presented as the mean ± SEM. Multiple group comparisons were made by one-way ANOVA with Bonferroni post hoc test. Comparisons between two groups were analyzed by unpaired 2-tailed Student's *t*-test with/without Welch's correction (determined by *F* test for equality of variances). A p-value <0.05 was considered statistically significant. Statistical analysis was performed by using Graph-Pad Prism software 8 and SPSS 28.

RESULTS

HDAC expression is altered in PBMCs from IPAH patients

We hypothesize that PH immunopathy involves epigenetic dysregulation in circulating immune cells. We examined the HDAC expression profile in PBMCs from IPAH patients (n=20) and healthy volunteers (n=15). Aberrant class II HDAC expression, i.e., increased HDAC 5, 6 and 9 levels, was observed in PBMCs from IPAH patients; decreased acetylated α-tubulin confirmed higher cytoplasmic HDAC6 activity. ($p<0.05$, adjusted for age and sex, Figure 1A; Figure E1A). In addition, IPAH PBMCs expressed higher tissue levels of inhibitor of matrix metalloproteinase-1 (TIMP-1) levels (Figure 1A), a biomarker related to high mortality in IPAH (19).

Reduced circulating Treg population in IPAH patients

We characterized the circulating lymphocyte composition by analyzing freshly isolated PBMCs with FACS. The proportion of Treg cells (defined by $CD3^+CD4^+CD25^+Foxp3^+$ lymphocytes) was reduced in IPAH patients (n=41; control n=37) and presented lowest in WHO functional class IV patients ($p<0.05$, adjusted for age and sex). No significant difference between patients and controls was observed in the percentage of major lymphocyte subsets, $CD3^+CD4^+$ (T helper cells), $CD3^+CD8^+$ (cytotoxic T cells) and $CD3^-CD19^+$ (B cells) (Figure E1B).

Programmed cell death-1 (PD-1) is an immune checkpoint against excess immune responses. PD-1/PD-L1 up-regulation is a recognized oncogenic signal, reflecting an immunocompromised microenvironment (20). Surface expression of PD-1 was up-regulated in circulating T cells from IPAH patients and the levels correlated negatively with Treg population ($r=-0.4157$, $p=0.0145$; $p=0.084$, adjusted for age and sex) (Figure 1C; Figure E1C).

SAHA induced the conversion of $Foxp3^+$ Tregs and differential gene expression in human conventional T cells from IPAH patients

HDACs are potent regulators of Treg function in humans (21). To evaluate whether there was a direct association between altered HDAC activities and Tregs in patients' PBMCs, we isolated conventional $CD4^+CD25^-$ T cells from IPAH patients and healthy volunteers and exposed them to SAHA. We found that patients' cells responded differently from controls.

SAHA treatment induced a significantly higher conversion of $Foxp3^+$ cells from conventional T cells in IPAH patients (266±61%) compared to healthy volunteers (107±22%, $p<0.05$, Figure 2A). In parallel, FOXP3 mRNA expression was significantly increased in IPAH (340±66% versus control 136±35%, $p<0.05$, Figure 2A).

We further sought to identify epigenetic-sensitive genes in IPAH immune cells that responded to SAHA. RNA sequencing of human $CD4^+CD25^-$ T cells demonstrated that SAHA treatment affected the transcription (adjusted $p<0.05$, Benjamini-Hochberg procedure) of 4241 genes in IPAH patients compared to 1429 genes in healthy volunteers (~2.5 times), suggesting that T cells from IPAH patients are more susceptible to SAHA treatment (Figure 2B and 2C).

GAGE/PANTHER analysis (http://www.pantherdb.org/) highlighted the "inflammation mediated by chemokine and cytokine signaling pathway" (P00031) in IPAH T cells (Figure E2A). The differentially expressed genes induced by SAHA in IPAH patients were annotated to biological pathways (KEGG) including immune response, metabolism, cell proliferation, vascular tone, and endocrine function (adjusted $p<0.1$, Figure 2D; Figure E2B). The key pathways impacted by SAHA treatment were validated by RT-qPCR (Figure E2C): ferroptosis (SLC3A2, FTH1, HMOX1), a newly recognized form of cell death as a critical regulator of immune cells; IL4 and IL10, two cytokines critically involved in Th1/Th2/Treg differentiation and T cell receptor signaling; NFKB2, RELA, RELB and XIAP, key elements in immune responses in NF-κB signaling; HIF1A, the master controller of glycolysis under hypoxic or

inflammatory stress; HDAC4, 5 and 7, class II HDACs; BRD4, acetyl-lysine-binding protein characterized in PH vasculopathy (22); and CTLA-4, CD28 and CD276, immune checkpoint molecules vital to Treg function (23). SAHA also modulated metabolic signaling pathways associated with PH pathogenesis, e.g., MAPK, cGMP-PKG and mTOR, as well as VEGF and vascular muscle contraction.

We further focused on the genes with ≧2-fold change. Gene ontology (GO) enrichment analysis related their molecular function to "binding" (36%) and "catalytic activity" (34%) (Figure 2E; Figure E2D). Histone acetylation is generally associated with transcription activation. Network analysis of protein-protein interactions by Reactome pathway analysis/NetworkAnalyst (networkanalyst.ca) revealed that the differentially up-regulated genes and their functional interactions were relevant to increased RNA polymerase II-dependent DNA binding of transcription factors involved in immune signaling pathway activation (Figure 2F), confirming the acetylation-related transcription activation in SAHA-treated T cells.

SAHA and VPA attenuated MCT-induced PH

We pursued HDAC-driven immune modulation by using SAHA (class I, II and IV) and VPA (class I HDAC) in monocrotaline (MCT)-induced PH rats. SAHA treatment attenuated elevated mean PAP, pulmonary arteriolar muscularization and RV hypertrophy (Figure 3A-D;

Figure E3A); by comparison, VPA was less effective (Figure E3B). Both SAHA and VPA reduced perivascular infiltration of $CD68^+$ monocytes/macrophages in the lungs (Figure 3E).

In MCT rat lungs, SAHA significantly increased bone morphogenetic protein receptor 2 (BMPR-2) expression (24) and reduced programmed death ligand 1 (PD-L1) expression (Figure 3F). Consistent with our previous studies (18), SAHA and VPA decreased Bcl-2 and survivin levels and SAHA increased p21 level (Figure 3G). Furthermore, SAHA reduced MCT-induced active MMP-2, MMP-9 (matrix metalloproteinase-2 and -9) and TIMP-1 (tissue inhibitor of metalloproteinase-1) expression in the lungs (Figure 3H) (25). Increased acetylated histones H3/H4 in HDACi-treated lungs confirmed HDAC inhibition (Figure E3C).

SAHA increased Th, Treg and NK populations along with increased histone acetylation and FOXP3 expression in PBMCs from MCT rats

We examined HDAC expression in PBMCs from MCT rats. Expression levels of HDAC1, 6 and 9 were increased but not HDAC5 or HDAC7 (Figure 4A; Figure E3D). MCT rats showed lower levels of circulating Th cells, Tregs and natural killer (NK) cells, which were reversed in SAHA-treated (but not VPA-treated) animals (Figure 4B).

SAHA increased acetylated histones H3/H4 and α-tubulin in PBMCs. Consistent with its class I HDAC inhibitory profile, VPA significantly increased acetylated H3, but not α-

tubulin (Figure 4C). The expression level of FOXP3, a key regulator of Treg activity, was reduced in MCT rat PBMCs and this was significantly reversed by SAHA (but not VPA) (Figure 4D). ChIP-qPCR revealed a significant enrichment of acetylated histone H4 in the FOXP3 promoter region in SAHA-treated rat PBMCs (Figure 4E).

SAHA attenuated PH phenotypes in SuHx rats

We validated the key findings from MCT rats in SuHx models, using male and female rats. SAHA treatment decreased the rise in PAP, RV hypertrophy and pulmonary vascular muscularization without significant systemic impacts; female rats seem to be more responsive to SAHA treatment (Figure 5A; Figure E4A). Cardiac MRI showed reduced RV mass, with preserved RV cardiac index and ejection fraction in SAHA-treated rats (Figure 5B and 5C), in line with a recent report that HDAC inhibition improved ventricular filling by reversing pre-existing diastolic dysfunction in hypertensive mice (26). Furthermore, SAHA significantly attenuated neointima formation and endothelial-to-mesenchymal transition (EndoMT), evidenced by decreased vimentin phosphorylation and Twist-1 expression in the lungs (Figure 5D) (27). SAHA increased BMPR-2 and decreased PD-L1 expression in SuHx rat lungs (Figure 5E).

SAHA increased circulating Tregs and NK populations in SuHx rats

Expression levels of HDAC1 and HDAC9, but not HDAC5 and 7, were increased in PBMCs from SuHx rats (Figure 6A; Figure E4B). HDAC6 levels were slightly increased ($p>0.05$); the acetylation levels of α-tubulin were significantly decreased in SuHx rats, reflecting increased HDAC6 activity (Figure E4C). The fractions of Th cells and Tregs in SuHx rats were decreased compared to healthy rats. SAHA selectively increased circulating $CD25^{+}Foxp3^{+}$ Tregs (but not Th cells) and NK cells in SuHx rats (Figure 6B-D; Figure E4D and E4E). Similar to IPAH patients, the percentage of PD-1^{+} T cells was significantly increased in SuHx rats, which was reversed by SAHA (Figure 6B-D). Interestingly, SAHA effects on increasing Treg and reducing PD-1^{+} T cells were stronger in female SuHx rats. Consistent with MCT rats, ChIP-qPCR confirmed the enrichment of acetylated histones H3/H4 bound to the FOXP3 promoter in PBMCs, linking HDAC inhibition to improved Treg function (Figure 6). Increased acetylation of histones H3/H4 in rat lungs verified HDAC inhibition in the treatment groups (Figure E4G).

Cytokine expression profile showed that IL-17, CXCL-10 and TIMP-1 expression were elevated in MCT and SuHx rat lungs, which were attenuated in VPA and SAHA-treated groups, suggesting suppressive effects of Th1 and Th17 responses in the lungs (Figure E5A).

Treg depletion in SuHx mice lessened the effects of SAHA on PH phenotypes

We speculated that the therapeutic effects of SAHA are attributed, at least in part, to the reconstitution of Treg population in PH rats. To address this, we used an anti-CD25 antibody to transiently deplete Tregs in SuHx mice, confirmed by FACS (>99% in Treg-depleted mice with or without SAHA treatment, Figure 7A).

In isotype-treated groups, SAHA treatment recovered Treg levels and significantly attenuated the SuHx-induced elevated RVSP, RV hypertrophy and pulmonary vascular remodeling, while the effect of SAHA on RVSP and pulmonary vascular remodeling was diminished in Treg-depleted animals (Figure 7B and 7C). It is interesting to note that the attenuation of RV hypertrophy by SAHA was not affected by Treg depletion. This may reflect that Tregs only take part in the therapeutic effects of SAHA on pulmonary vascular remodeling. The direct cardiac protective effects of SAHA may also associate with other pathways, e.g., MEF2 (myocyte enhance factor 2) activation which plays a key role in the preservation of RV function; suppressing cardiac fibroblast activation which reverses pre-existing diastolic dysfunction. (14, 28, 29). In addition, anti-PD-1 treatment did not significantly improve the established PH hemodynamics and pulmonary pathology in SuHx mice (Figure E6).

SAHA and VPA inhibit inflammatory mediator release and leukocyte migration

The immune modulatory effects of SAHA might not only impact immune cells but vascular cells. Immune-vascular interactions play a significant role in the pathogenesis of PAH.

We tested the effects of HDAC inhibition on cytokine release from TNF-α-stimulated HPAECs and then PBMC chemotaxis, mimicking immune cell recruitment from inflammatory signals from pulmonary endothelium. TNF-α stimulated cytokines/chemokines release in HPAECs, several of which have been previously reported relevant to human PAH, including CXCL-10, CXCL-11, RANTES, C5/C5a, IL-6, GM-CSF and sICAM-1 (30). SAHA treatment reduced the up-regulated cytokines levels; in comparison, VPA had limited effect (Figure 8A). Quantitative PCR confirmed that SAHA and VPA attenuated TNF-α-induced transcriptional expression of CXCL10, CXCL11 and NF-κB subunits, RELA and NFKB1 (Figure 8B). In the functional assay, SAHA and VPA prevented PBMC migration in response to chemoattractant signals from TNF-α-stimulated HPAECs (Figure 8C).

DISCUSSION

This study reveals a pivotal role for $Foxp3^+$ regulatory T cells in the pathology of PAH and the opportunity to intervene pharmacologically by HDAC-dependent epigenetic modulation. We report an IPAH immune phenotype, characterized by reduced peripheral $CD25^+Foxp3^+$ Treg cells and increased immune checkpoint PD-1 expression in circulating T cells. Immune cells from these patients showed increased HDAC 5, 6 and 9 expression and decreased α-tubulin acetylation. In addition, T cells from IPAH patients exhibited a cluster of epigenetic-sensitive genes involved in the immune regulatory network and treatment with

HDAC inhibitor, SAHA, differentially modified these genes and induced Foxp3-dependent Treg conversion. Rodent PH models resembled HDAC aberrations and T cell dysfunction. SAHA treatment restored circulating $Foxp3^+$ Treg numbers, reduced extracellular matrix enzymatic activities, up-regulated BMPR-2 and down-regulated PD-L1 in PH rat lungs. In SuHx mice, transient Treg-specific depletion by anti-CD25 antibody diminished the beneficial effects of SAHA on PH phenotype. SAHA inhibited TNF-α induced PH-related cytokine/chemokine release from HPAECs in culture and immune cell chemotaxis.

Aberrant HDAC expression is well recognized to cause an imbalance in histone acetylation, which consequently alters chromatin accessibility and transcriptional activity, contributing to persistent cell phenotypes in various diseases including PAH (31). Profiling HDACs pattern in circulating PBMC helped to define specific 'epigenetic cell memories' in PAH patients; for example, Potus et al. recently reported aberrant expression of the epigenetic regulator, TET2, in PBMCs from PAH patients in a large-scale cohort (32).

Circulating $Foxp3^+$ Tregs were reduced in IPAH patients, most pronounced in WHO functional class IV patients. Tregs regulate immune responses by inhibiting the proliferation and modifying the function of effector T and B cells, monocytes/macrophages, dendritic and NK cells (10, 33). Impairment of Tregs and disproportion of Tregs/Th17 cells are inflammatory signatures, correlating with prognosis in IPAH, connective tissue disease and chronic obstructive pulmonary disease associated PAH (5, 6, 34). A multigene panel composed of 25

Treg-related genes was recently identified in PAH patient lungs (35). Of note, several studies reported increased peripheral $CD3^+CD4^+CD127^{low}$ Treg numbers in PAH patients (36–38), while our data related Treg dynamics to the immune status along the progression of PH and the degree of autoimmunity involved in PH development. The expanded Treg subset in PAH was shown non-functional with low Foxp3 activity (39). Reduced numbers of $Foxp3^+$ cells in IPAH patient lungs suggest impaired Treg trafficking, which may be also involved (40). Accumulating preclinical evidence has shown that recovering abnormal Tregs may protect PAH by interacting with other immune cells to impact pulmonary vascular cells (41). Athymic Treg-absent rats exhibit exaggerated pulmonary vascular remodeling and inflammatory infiltration following Sugen5416 injection, whilst Treg reconstitution attenuates this phenotype (8, 42).

HDAC inhibition boosts Tregs (15). SAHA treatment induced more pronounced Foxp3 expression in IPAH conventional T cells and Treg conversion *ex vivo*; among these patients, a subgroup appeared to be super-responsive to SAHA. The higher susceptibility to HDAC inhibition in IPAH T cells was associated with a set of differentially expressed genes, particularly those genes involved in immune, metabolism and vascular homeostasis. This may reflect the epigenetic-programmed cell phenotypes and memories in IPAH T cells. In the gene sets, SAHA differentially modified several known PH-relevant genes, e.g., down-regulating BRD4, TIMP1, CFP, CFB, NRP1 and SERPINA1 and up-regulating CFH. Upregulated BRD4,

a recognized histone acetylation reader, was associated with Bcl-2, survivin, p21 and NFAT in PAH lungs (22). Increased TIMPs and NRP1 and reduced inhibitory factor H (CFH) were recently shown to predict the survival of IPAH patients (19). Functional enrichment analysis further associated these differentially up-regulated genes with DNA-binding transcription factor activity, providing evidence of comprehensive chromatin relaxation and subsequent transcription reprogramming. HDACi were first introduced to clinical application for cancer therapy on the grounds that the unique epigenetic modifications/signatures are the "Achilles Heels" of the transformed cells (43). The presence of potential super-responders in our study mirrors this concept; the specific alternations of the HDAC-sensitive genes define immune cell memory/addiction in PH. Our data indicate the importance of developing epigenome-based approaches to target this "epigenetic vulnerability" in PH.

HDACi treatment attenuated PH phenotypes in MCT and SuHx rat models. In both PH models, SAHA treatment restored the decreased population of circulating Tregs, accompanied by enrichment of acetylated H3/H4 in the FOXP3 promoter region and increased FOXP3 mRNA expression. The results are consistent with a previous report that histone acetylation regulates constitutive FOXP3 activation, promoting Treg population in T cells isolated from healthy donors (44). PBMCs from IPAH patients and PH rats exhibit aberrant HDAC9 expression and HDAC6 activity in common (Table E1). HDAC9 is involved in the process of histone deacetylation at the FOXP3 locus and HDAC6 directly deacetylate Foxp3, increasing

Foxp3 susceptibility for degradation (45–47). This may explain the better efficiency of SAHA than VPA. Furthermore, we observed that female SuHx rats were more responsive to SAHA treatment in attenuating PH phenotypes and restoring Tregs. Treg abnormalities have been featured in other female-predominant diseases in addition to PAH, such as systemic lupus erythematosus; X-linked FOXP3 regulation and associated hormonal fluctuations may underlie the gender differences (48). Females athymic rats developed more severe PH than males and Treg reconstitution exerted a more dominant protective function in females (42). Our data suggested a role of HDAC regulation in sex differences in PH, which involves Treg function. Induction of intrinsic Treg activity has emerged as a promising approach for treating diseases with overactive immune responses (49). We conducted further studies in Treg-depleted mice. The effects of SAHA on SuHx-induced pulmonary pathology were significantly reduced in this model, arguing for the direct involvement of Tregs for HDAC-targeted modulations in PH.

In addition, SAHA treatment increased the NK cell population in PH rats. NK cells play a regulatory role in reparative immunity and vascular integrity; deficient NK cells with elevated production of MMP-9 have been shown in human and animal PH (50). SAHA treatment consistently exhibited anti-inflammatory effects whether directly by suppressing Th1/Th17 or via Treg induction or both; in TNF-α stimulated HPAECs, SAHA limited immune cell recruitment through inhibiting cytokine release; in PH rat lungs, there were reduced levels of IL-17, CXCL-10 and TIMP-1 expression in SAHA-treated rats, suggesting suppressive effects

on Th1 and Th17 responses (51). These data are in line with the protective effects of SAHA on pulmonary remodeling by reducing extracellular matrix enzymatic activity, e.g., MMP-2 and MMP-9, along with proliferative factors, e.g., Bcl-2 and survivin.

Intriguingly, we observed an increased circulating PD-1^{+}T cell population in IPAH patients, in accordance with a recent report from 25 treatment-naïve IPAH patients (52). Increased PD-1^{+} population among circulating T cells may signify excessive T cell activation and subsequent exhaustion in chronic inflammatory disorders, e.g., multiple sclerosis (53), COVID-19 pneumonia (54, 55), and idiopathic pulmonary fibrosis (56, 57) In IPAH patients, increased PD-1^{+} T cells together with reduced Treg population indicated over-activation of pro-inflammatory T cells (58). PH rats recapitulated the immunophenotype of increased circulating PD-1^{+} T cells with elevated PD-L1 expressions in the lungs, which was reversed in the SAHA-treated groups. In the *ex vivo* IPAH T cells, SAHA also selectively modulated PD-1 regulators including NFATc1, NF-κB, and TBX21. Recent clinical studies reported adverse effects of anti-PD-1 therapies on RV function and pulmonary circulation (59). We conducted selective PD-1 blockade in SuHx mice and didn't observe a significant impact on PH phenotypes (Figure E6). These data support that the increased PD-1^{+} T cells are likely a consequence or feedback of the T cell over-activation rather than a primary cause in PH.

There are several limitations in this study. The blood collection date differs from the pulmonary catheterization date in the IPAH patients, which limits the data correlation of

HDAC expression and PD-1/Treg population with the hemodynamic measurements. The relationship to clinical treatments could not be determined in patients due to various treatment combinations. Tregs represent approximately 1-4% of peripheral blood PBMCs. Therefore, it is challenging to further define the HDAC expression in these cells or its PD-1^+ or CTLA-4^+ subsets. Considering specific FOXP3-depleted models such as FOXP3-DTR (diphtheria toxin receptor) mice having a short lifespan (60), we used CD25 antibodies to establish experimental Treg-depleted mice.

In summary, we highlight a novel epigenetic mechanism in modulating Treg function in PAH (Figure 9) – the restoration of $Foxp3^+$ Treg population/function by HDAC inhibition is crucial in resolving PAH pathology. The measurable HDAC expression pattern and activity in accessible circulating immune cells, along with PD-1^+ T cell and $Foxp3^+$ Treg population/function, are potential biomarkers representing the immune status of patients.

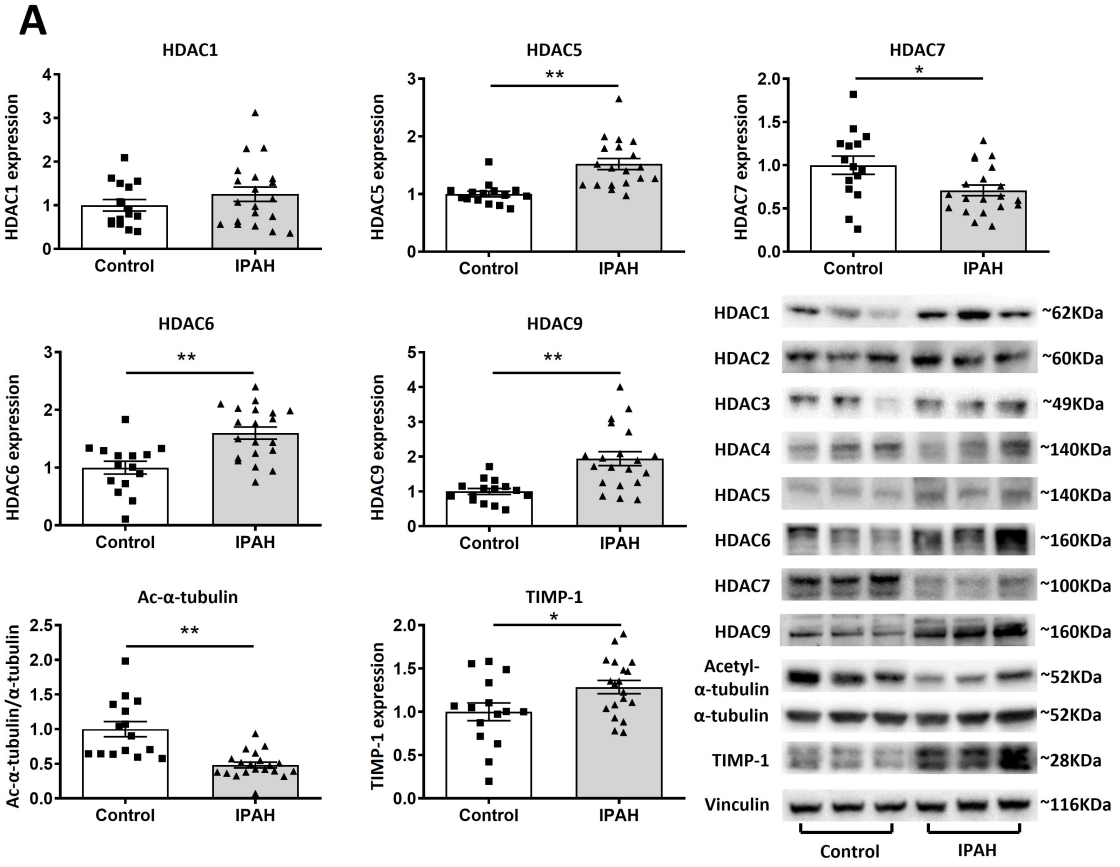
Author contributions: L.Z. and C-N.C. developed concepts and experimental designs. C-N.C. conducted the experiments, assisted by F-C.Y. and C-Y.X. N.H. supervised epigenetic analysis. C-N.C and S.R. performed ChIP-qPCR assay. S.A. and J.W. organized human blood sample collection. N.B. and Lin Z. performed the cardiac MRI. Y-G.C. assisted with proteome cytokine assay. M.G.F. and K.R.S. performed immunofluorescent staining with rat CD68. P.C. and S.S.P. performed RT-qPCR in HPAECs. N.H. and Lin Z. assisted with RNA-sequencing analysis. C-N.C. performed data analysis and assembled the figures. L.Z. and C-N.C. interpreted the data and wrote the manuscript., revised by M.R.W.

Acknowledgments: This research was supported by a project grant from British Heart Foundation PG/18/2/33446.

Table 1: Clinical Characterization of IPAH Patients.

	IPAH (n=41)	Control (n=37)
Age, year-old	54 (42.5-69)	52 (38.5-59)
Sex (M:F), n	13:28	11:26
Ethnic origin, White British/Asian/other	31/4/6	28/5/4
WHO functional class I/II/III/IV, n	0/10/24/7	
6MWD, m	320 (176-380)	
Treatment		
Treatment naïve	0	
Monotherapy (ERA of PDEI5)	8	
Dual-combination therapy	21	
Triple-combination therapy	12	
CCB for vosoresponders yes/no, n	4/37	
Warfarin yes/no, n	33/8	
Haemodynamic charecteristics		
Mean PA pressure, mmHg	51.0 (38.8-61.0)	
PA wedge pressure, mmHg	12.0 (8.5-15.0)	
Mean RV pressure, mmHg	9.0 (5.0-12.0)	
Cardiac output, L/min	4.3 (3.2-5.8)	

The data are presented as median (25^{th}-75^{th} percentile). M: male; F: female; 6MWD: 6-minute walk distance; ERA: endothelin receptor antagonist; PDEI5: phosphodiesterase-5 inhibitor; WHO: world health organization; PA: pulmonary artery; RV: right ventricle; CCB: calcium channel blocker.


A
HDAC1
HDAC1 expression
Control
IPAH
HDAC5
HDAC5 expression
**
HDAC7
HDAC7 expression
*
HDAC6
HDAC6 expression
HDAC9
HDAC9 expression
Ac-α-tubulin
Ac-α-tubulin/α-tubulin
TIMP-1
TIMP-1 expression
HDAC1 ~62KDa
HDAC2 ~60KDa
HDAC3 ~49KDa
HDAC4 ~140KDa
HDAC5 ~140KDa
HDAC6 ~160KDa
HDAC7 ~100KDa
HDAC9 ~160KDa
Acetyl-α-tubulin ~52KDa
α-tubulin ~52KDa
TIMP-1 ~28KDa
Vinculin ~116KDa

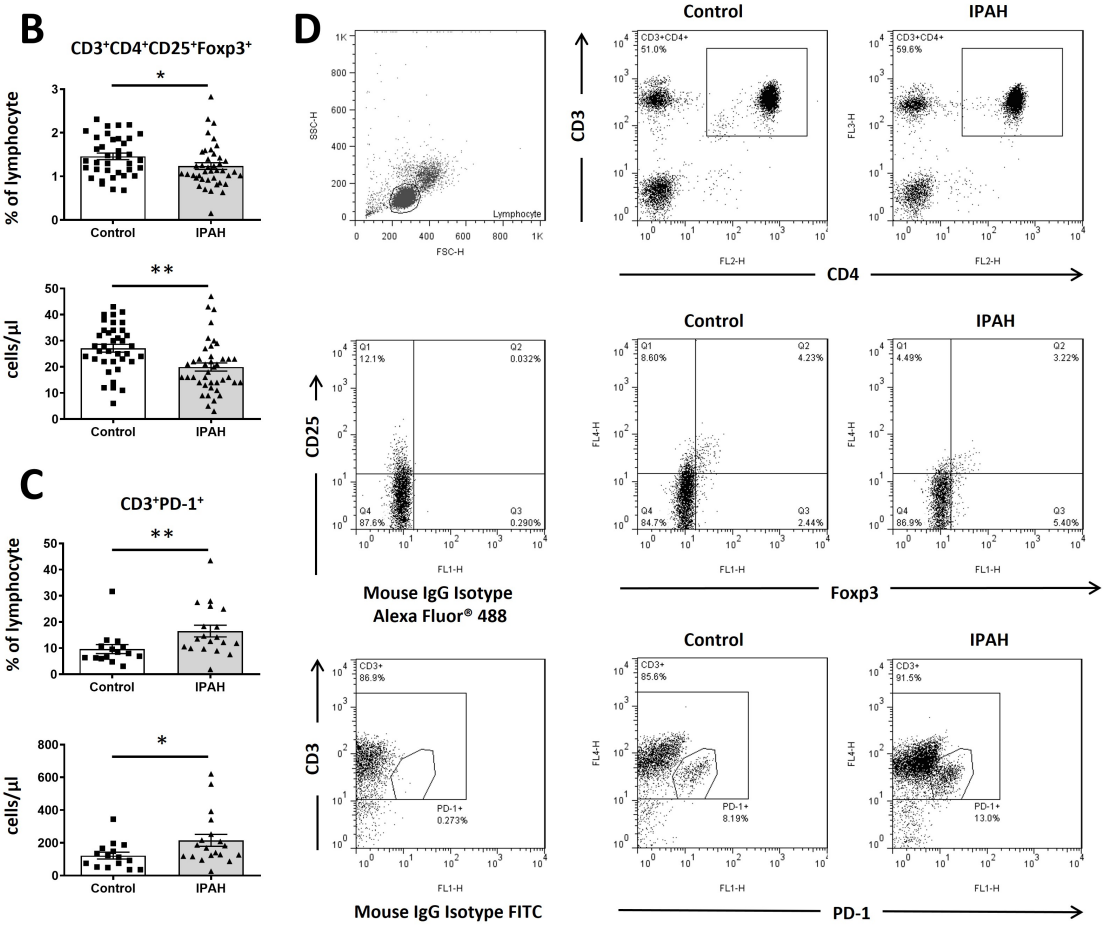
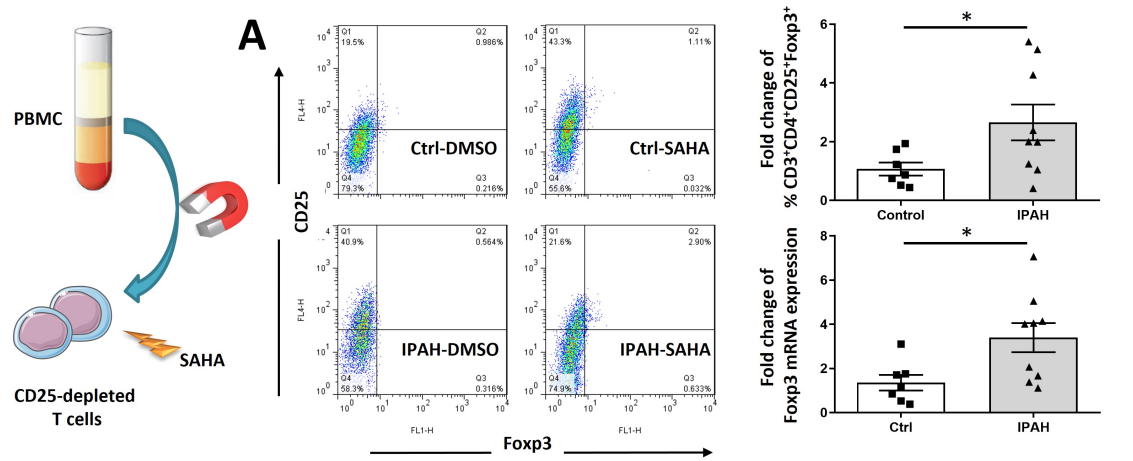
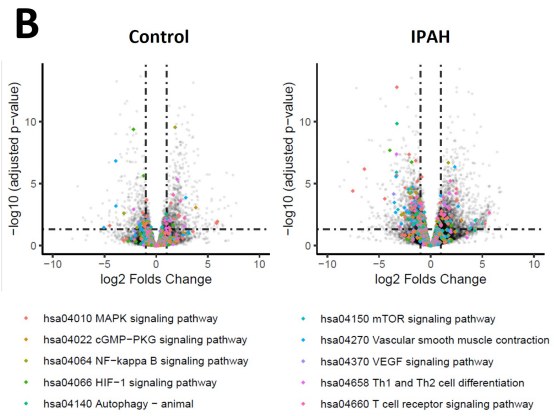
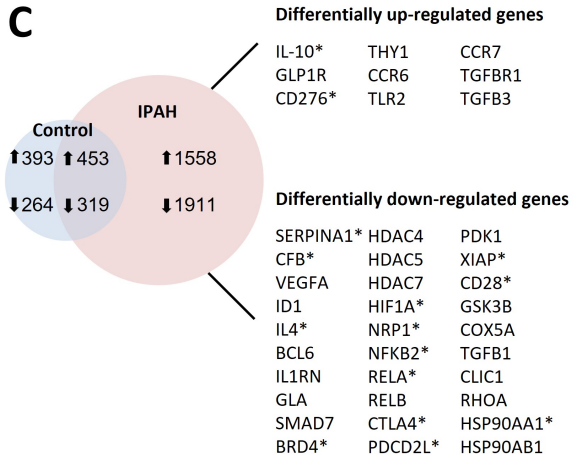
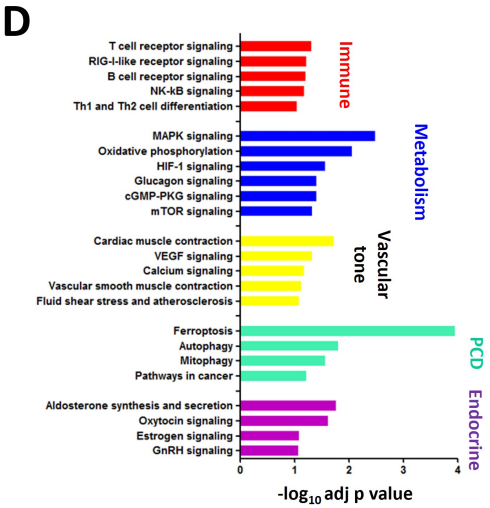

B
CD3+CD4+CD25+Foxp3+
% of lymphocyte
cells/μl
C
CD3+PD-1+
D
Control
IPAH
CD3
CD4
CD25
Foxp3
Mouse IgG Isotype
Alexa Fluor® 488
Mouse IgG Isotype FITC
PD-1

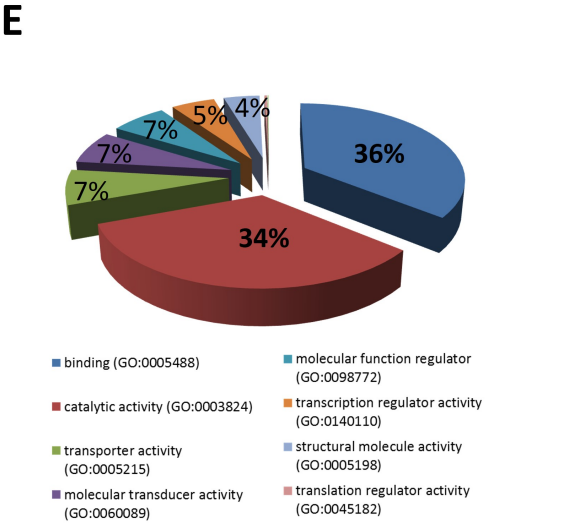
Figure 1. HDAC expression levels in human PBMCs along with Treg and $CD3^+PD\text{-}1^+$ cell population were changed in IPAH patients. Protein expression levels of **A**, HDAC1, HDAC5, HDAC6, HDAC7, HDAC9, acetylated α-tubulin and TIMP-1 in human PBMCs, with representative immunoblots. The data were generated from optical density measurements of individual bands normalized to vinculin (acetylated α-tubulin to total α-tubulin) and presented as fold change relative to control group. n=15 in control and n=20 in IPAH. **B**, The percentages in total lymphocytes and actual cell counts of circulating Treg ($CD3^+CD4^+CD25^+Foxp3^+$) cells of control subjects (n=37) and IPAH patients (n=41). **C**, The percentages and actual cell counts of circulating $CD3^+PD\text{-}1^+$ cell population of control subjects (n=15) and IPAH (n=19). Control: healthy volunteer; IPAH: idiopathic pulmonary arterial hypertension patient. * $p<0.05$, ** $<p<0.01$, adjusted for age and sex. **D**, FSC/SSC gating and representative dot plots of FACS analysis.


A
PBMC
SAHA
CD25-depleted
T cells
CD25
Foxp3
Ctrl-DMSO
Ctrl-SAHA
IPAH-DMSO
IPAH-SAHA
Fold change of
% CD3+CD4+CD25+Foxp3+
Control
IPAH
Fold change of
Foxp3 mRNA expression
Ctrl
IPAH


B
Control
IPAH
−log10 (adjusted p−value)
log2 Folds Change
hsa04010 MAPK signaling pathway
hsa04022 cGMP−PKG signaling pathway
hsa04064 NF−kappa B signaling pathway
hsa04066 HIF−1 signaling pathway
hsa04140 Autophagy − animal
hsa04150 mTOR signaling pathway
hsa04270 Vascular smooth muscle contraction
hsa04370 VEGF signaling pathway
hsa04658 Th1 and Th2 cell differentiation
hsa04660 T cell receptor signaling pathway


C
Differentially up-regulated genes
IL-10* THY1 CCR7
GLP1R CCR6 TGFBR1
CD276* TLR2 TGFB3
Control
IPAH
⬆393 ⬆453 ⬆1558
⬇264 ⬇319 ⬇1911
Differentially down-regulated genes
SERPINA1* HDAC4 PDK1
CFB* HDAC5 XIAP*
VEGFA HDAC7 CD28*
ID1 HIF1A* GSK3B
IL4* NRP1* COX5A
BCL6 NFKB2* TGFB1
IL1RN RELA* CLIC1
GLA RELB RHOA
SMAD7 CTLA4* HSP90AA1*
BRD4* PDCD2L* HSP90AB1


D
T cell receptor signaling
RIG-I-like receptor signaling
B cell receptor signaling
NK-kB signaling
Th1 and Th2 cell differentiation
Immune
MAPK signaling
Oxidative phosphorylation
HIF-1 signaling
Glucagon signaling
cGMP-PKG signaling
mTOR signaling
Metabolism
Cardiac muscle contraction
VEGF signaling
Calcium signaling
Vascular smooth muscle contraction
Fluid shear stress and atherosclerosis
Vascular tone
Ferroptosis
Autophagy
Mitophagy
Pathways in cancer
PCD
Aldosterone synthesis and secretion
Oxytocin signaling
Estrogen signaling
GnRH signaling
Endocrine
-log10 adj p value


E
36%
34%
7%
7%
7%
5%
4%
binding (GO:0005488)
catalytic activity (GO:0003824)
transporter activity (GO:0005215)
molecular transducer activity (GO:0060089)
molecular function regulator (GO:0098772)
transcription regulator activity (GO:0140110)
structural molecule activity (GO:0005198)
translation regulator activity (GO:0045182)

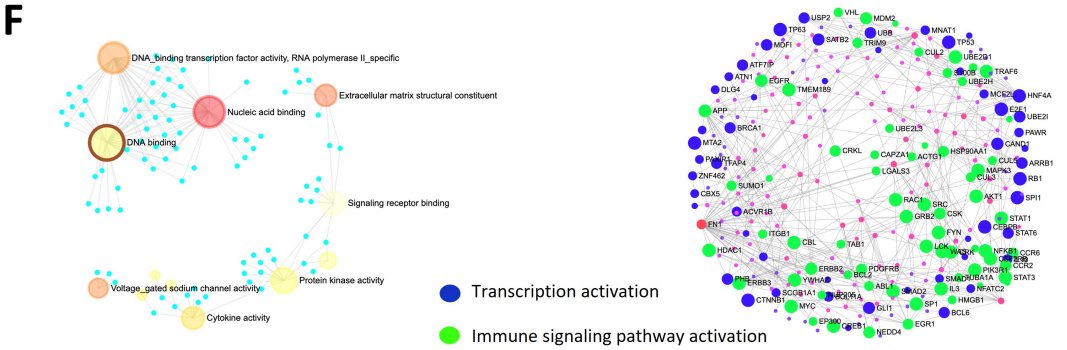

F
DNA binding transcription factor activity, RNA polymerase II specific
Extracellular matrix structural constituent
Nucleic acid binding
DNA binding
Signaling receptor binding
Protein kinase activity
Voltage gated sodium channel activity
Cytokine activity
Transcription activation
Immune signaling pathway activation

Figure 2. SAHA preferentially induced *ex vivo* conversion of $CD4^+CD25^-$ T cells from IPAH patients to $Foxp3^+$ Tregs, accompanied by selective transcriptional regulation. Isolated $CD4^+CD25^-$ T cells from IPAH patients (n=9) and healthy donors (n=7) were treated with either SAHA (500nM) or DMSO (untreated) for 6 days and analyzed by **A**, FACS quantification of $CD3^+CD4^+CD25^+Foxp3^+$ cells and RT-qPCR for FOXP3 expression (normalized to GAPDH). The data were presented as the fold change over the DMSO group from the same subject. Control: healthy donor; IPAH: idiopathic pulmonary arterial hypertension patient. * $p<0.05$. **B**, Transcriptome analysis (n=3) of gene sets differentially altered upon SAHA treatment in $CD4^+CD25^-$ T cells was performed by GAGE analysis and presented in the volcano plot. **C**, Venn diagram indicated a significantly higher number of altered genes in response to SAHA treatment in $CD4^+CD25^-$ T cells from IPAH patients (4241 genes, up-regulation of 2011 genes and down-regulation of 2230 genes) in comparison to healthy donors (1429 genes, up-regulation of 846 genes and down-regulation of 583 genes). We highlight the key molecules/pathways impacted by SAHA treatment relevant to PH. **D**, The most significantly modified pathways (KEGG) involved in these differentially altered genes are immune, metabolism, vascular tone, programmed cell death (PCD) and endocrine. FDR-adjusted p values were calculated using Benjamini and Hochberg procedure. **E**, Pie chart presented the distribution of molecular function of the differentially altered genes with >2-fold changes by SAHA in IPAH T cells, indicating the association mainly with "binding" (36%) and "catalytic activity" (34%). **F**, Reactome /Networkanalyst analysis of the differentially up-regulated genes (>2-fold changes) showed t top 9 clusters with their representative enriched term presented in the left panel and the predicted protein-protein interaction presented in the right panel.

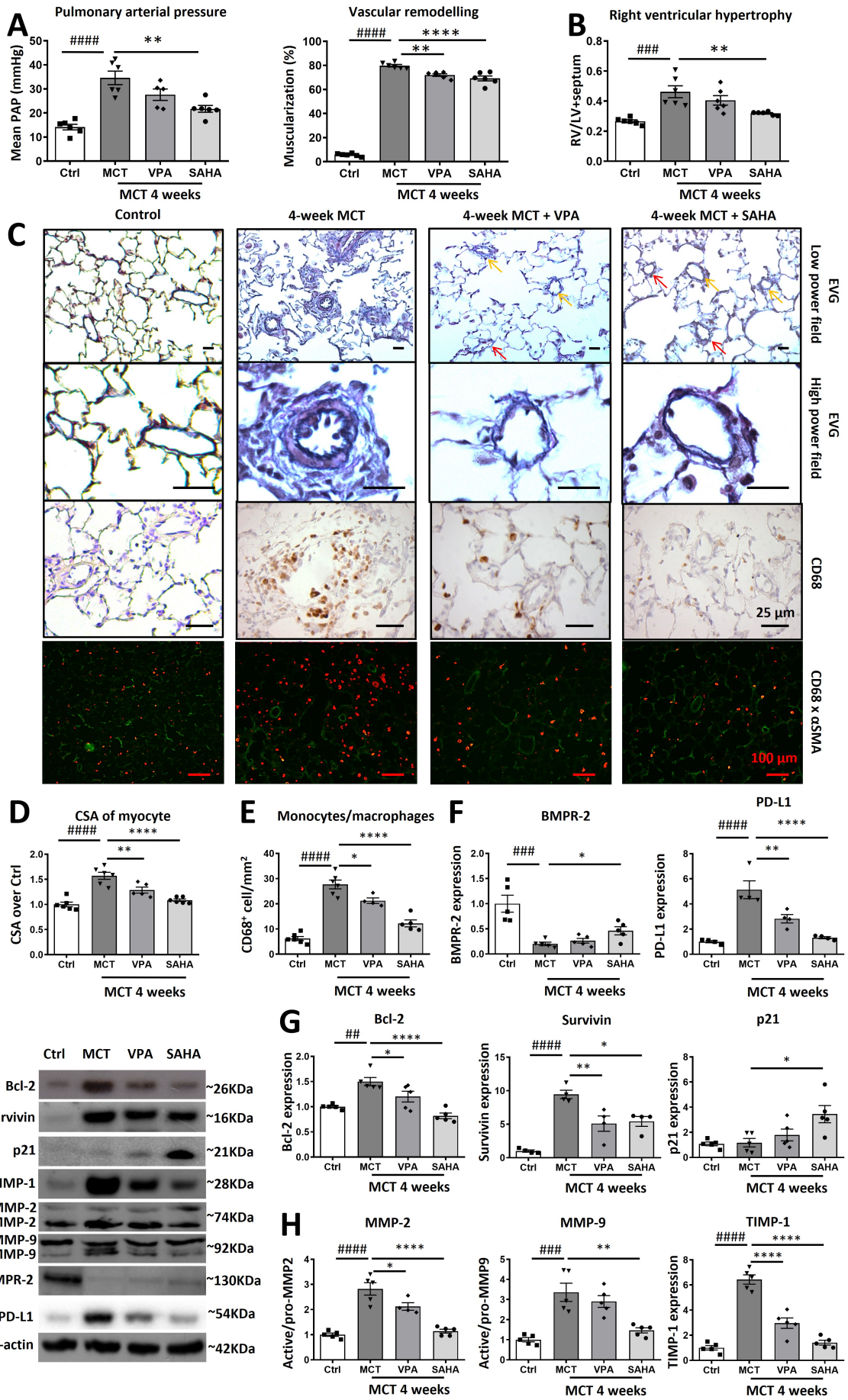

A
Pulmonary arterial pressure
Mean PAP (mmHg)
Vascular remodelling
Muscularization (%)
B
Right ventricular hypertrophy
RV/LV+septum
Ctrl
MCT
VPA
SAHA
MCT 4 weeks
C
Control
4-week MCT
4-week MCT + VPA
4-week MCT + SAHA
EVG
Low power field
High power field
CD68
CD68 x αSMA
25 μm
100 μm
D
CSA of myocyte
CSA over Ctrl
E
Monocytes/macrophages
CD68+ cell/mm2
F
BMPR-2
BMPR-2 expression
PD-L1
PD-L1 expression
Ctrl MCT VPA SAHA
Bcl-2 ~26KDa
Survivin ~16KDa
p21 ~21KDa
TIMP-1 ~28KDa
pro MMP-2 MMP-2 ~74KDa
pro MMP-9 MMP-9 ~92KDa
BMPR-2 ~130KDa
PD-L1 ~54KDa
β-actin ~42KDa
G
Bcl-2
Bcl-2 expression
Survivin
Survivin expression
p21
p21 expression
H
MMP-2
Active/pro-MMP2
MMP-9
Active/pro-MMP9
TIMP-1
TIMP-1 expression

Figure 3. SAHA and VPA attenuated established MCT-induced pulmonary hypertension in rats in association with reduction of inflammatory and proliferative factors. A, Mean pulmonary artery pressure (PAP) and the percentage of muscularised vessels with the representative lung sections (low power field x200 and high power field x400) stained with elastic van Gieson (EVG). **B**, Right ventricular hypertrophy (RVH) quantified by RV/LV+septum ratio (Fulton index). **C**, The immunohistochemistry images of lung sections from MCT rats stained with EVG, red arrows refer to non-muscularized vessels whereas yellow arrows refer to partially muscularized vessels; immunohistochemistry of CD68 and immunofluorescent images of lung sections with CD68 (red) and α-smooth muscle actin (green). **D**, Quantification of average cross-sectional area (CSA) of RV myocyte. E, Quantification of $CD68^+$ cell count in the rat lungs. Protein expression levels of **F**, BMPR-2 and PD-L1. **G**, Bcl-2, Survivin and p21. **H**, MMP-2, MMP-9 and TIMP-1, in lung homogenates of MCT rats. The data were generated from optical density measurements of individual bands normalized to β-actin and presented as fold change relative to Ctrl. MMP-2 and MMP-9 were presented as the ratio of "active" bands over "pro" bands. Ctrl: healthy control; MCT: MCT for 4 weeks; VPA: MCT with VPA 300 mg/kg/day, and SAHA: MCT with SAHA 50 mg/kg/day. The data are presented as mean± SEM. n=4 to 6 for each group. *p<0.05, ** p<0.01, *** p<0.001, **** p<0.0001 compared with MCT; ## p<0.01, ### p<0.001, #### p<0.0001 compared with Ctrl.

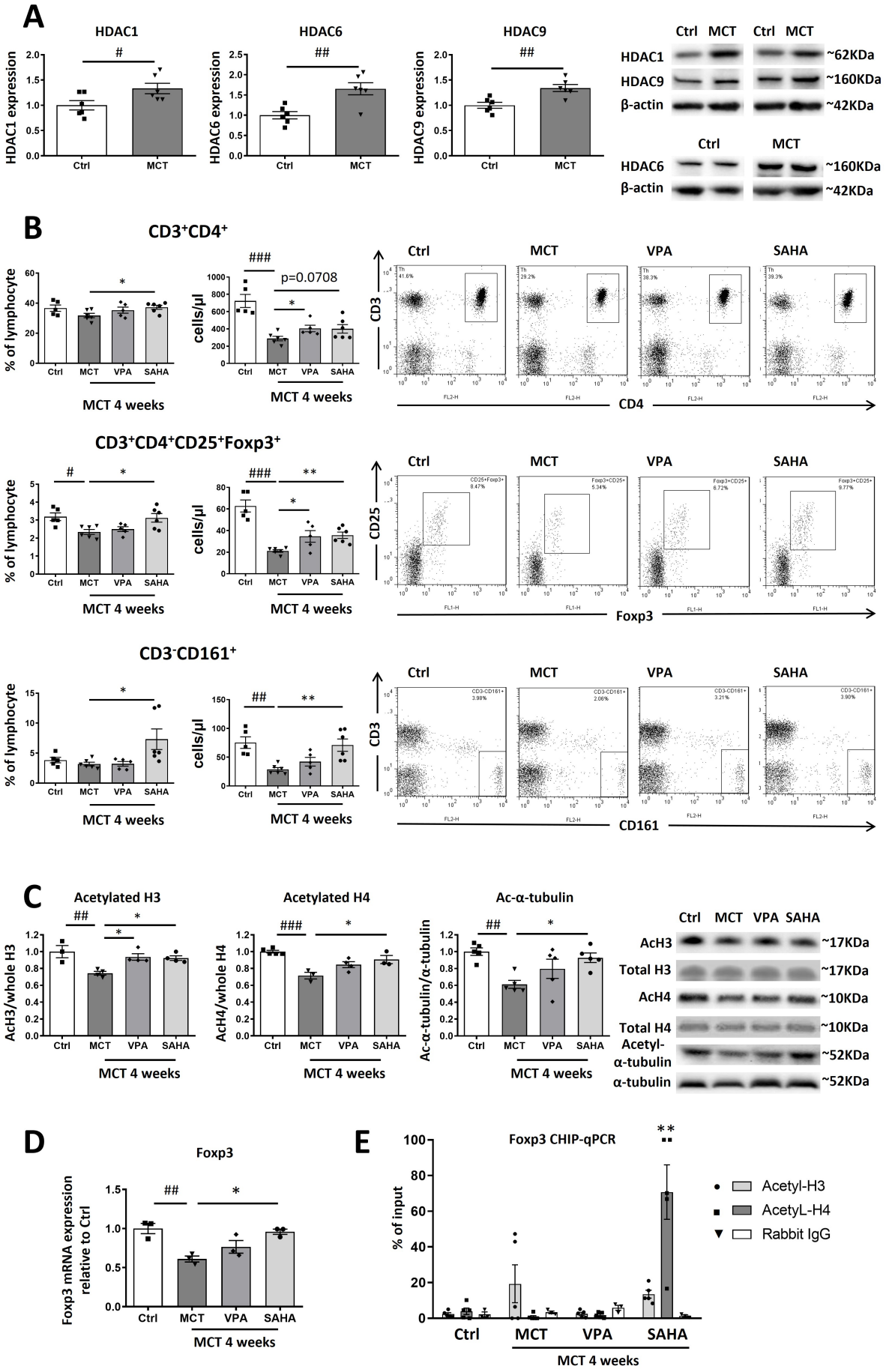

A
HDAC1
HDAC6
HDAC9
HDAC1 expression
HDAC6 expression
HDAC9 expression
Ctrl
MCT
Ctrl MCT Ctrl MCT
HDAC1
HDAC9
β-actin
~62KDa
~160KDa
~42KDa
Ctrl MCT
HDAC6
β-actin
~160KDa
~42KDa
B
CD3+CD4+
% of lymphocyte
cells/μl
p=0.0708
Ctrl MCT VPA SAHA
MCT 4 weeks
CD3
CD4
CD3+CD4+CD25+Foxp3+
CD25
Foxp3
CD3-CD161+
CD161
C
Acetylated H3
Acetylated H4
Ac-α-tubulin
AcH3/whole H3
AcH4/whole H4
Ac-α-tubulin/α-tubulin
Ctrl MCT VPA SAHA
AcH3
Total H3
AcH4
Total H4
Acetyl-α-tubulin
α-tubulin
~17KDa
~17KDa
~10KDa
~10KDa
~52KDa
~52KDa
D
Foxp3
Foxp3 mRNA expression relative to Ctrl
E
Foxp3 CHIP-qPCR
% of input
Acetyl-H3
AcetyL-H4
Rabbit IgG

Figure 4. SAHA rescued circulating Th, Treg and NK populations in MCT rats in line with increased histone acetylation and FOXP3 expression in PBMCs. A, HDAC1, HDAC6 and HDAC9 expression levels in PBMCs from MCT rats. The data were generated from optical density measurements of individual bands normalized to β-actin and presented as fold change relative to Ctrl. **B**, The percentages in total lymphocytes and actual cell counts of circulating Th ($CD3^+CD4^+$), Treg ($CD3^+CD4^+CD25^+Foxp3^+$) and NK ($CD3^-CD161^+$) cell population of MCT rats. **C**, Acetylated H3, acetylated H4 and acetylated α-tubulin expression levels in PBMCs from MCT rats. The data were generated from optical density measurements of individual bands normalized to total H3/H4 or α-tubulin and presented as fold change relative to Ctrl. **D**, FOXP3 mRNA expression in PBMCs from MCT rats. **E**, ChIP pull-down of anti-acetylated H3/H4-associated chromatin, followed by qPCR for FOXP3 promoter. The data were quantified as the percentage of the input levels. Ctrl: healthy control; MCT: MCT for 4 weeks; VPA: MCT with VPA 300 mg/kg/day, and SAHA: MCT with SAHA 50 mg/kg/day. n= 4 to 6 for each group. * $p<0.05$, ** $p<0.01$ compared with MCT; # $p<0.05$, ## $p<0.01$, ### $p<0.001$ compared with Ctrl.

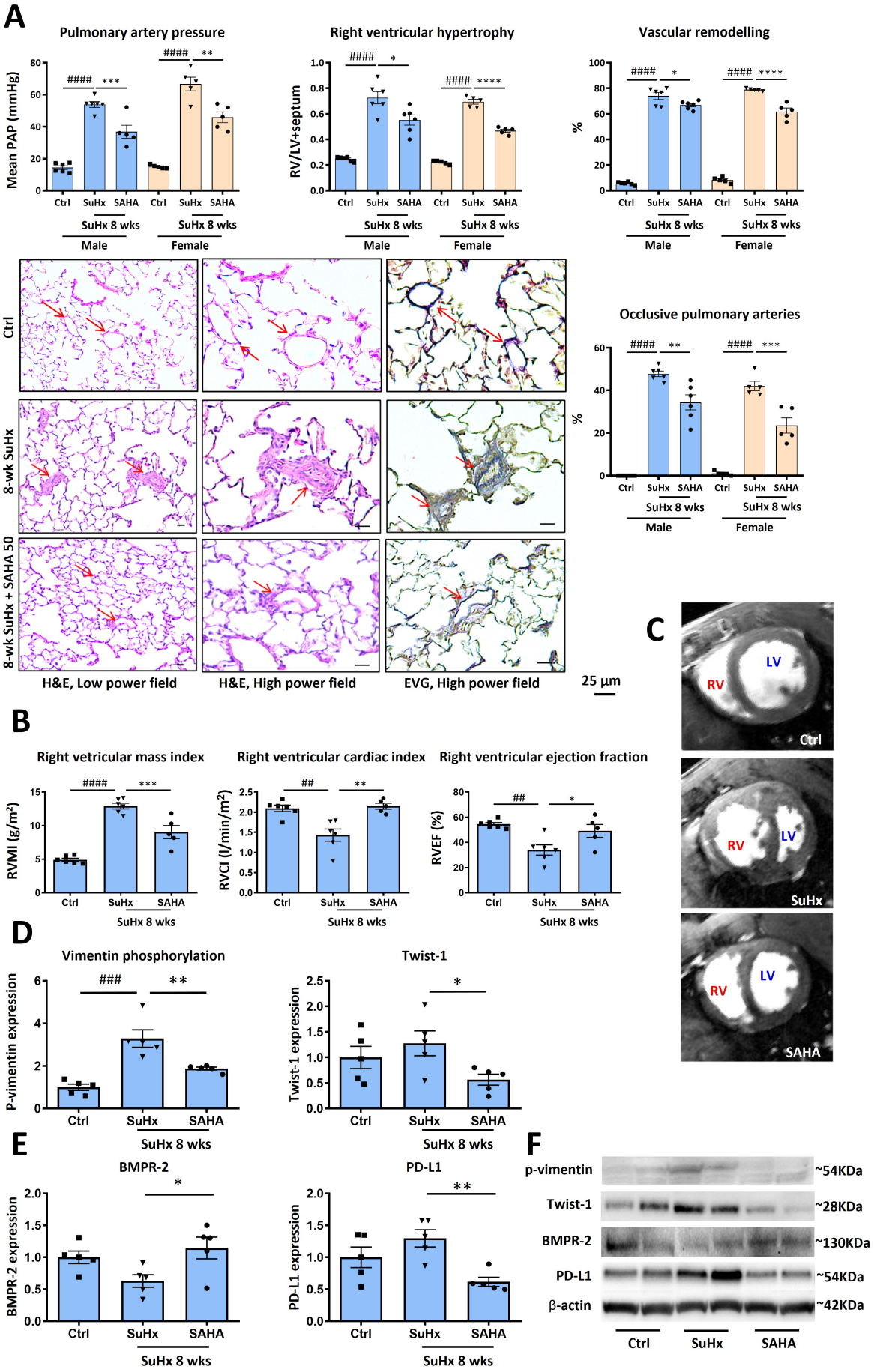

A
Pulmonary artery pressure
Mean PAP (mmHg)
Right ventricular hypertrophy
RV/LV+septum
Vascular remodelling
%
Ctrl
SuHx
SAHA
SuHx 8 wks
Male
Female
Occlusive pulmonary arteries
8-wk SuHx
8-wk SuHx + SAHA 50
H&E, Low power field
H&E, High power field
EVG, High power field
25 μm
B
Right vetricular mass index
RVMI (g/m²)
Right ventricular cardiac index
RVCI (l/min/m²)
Right ventricular ejection fraction
RVEF (%)
C
LV
RV
D
Vimentin phosphorylation
P-vimentin expression
Twist-1
Twist-1 expression
E
BMPR-2
BMPR-2 expression
PD-L1
PD-L1 expression
F
p-vimentin
Twist-1
BMPR-2
PD-L1
β-actin
~54KDa
~28KDa
~130KDa
~54KDa
~42KDa

Figure 5. SAHA attenuated established SuHx-induced pulmonary hypertension in rats in association with induction of BMPR-2 and reduction of PD-L1 in the lungs. A, Mean pulmonary artery pressure (PAP), right ventricular hypertrophy (RVH) quantified by RV/LV+septum ratio (Fulton index), the percentage of muscularised vessels and occluded vessels (diameter <50μm); representative images of lung sections stained with hematoxylin-eosin and elastic van Gieson (low power field x200 and high power field x400). Blue columns represent male rats (n=6); pink columns represent female rats (n=5). **B**, The quantification of MR data presented as RV mass index (RVMI), RV cardiac index (RVCI) and RV ejection fraction (RVEF), and **C**, Representative images of short-axis cardiac MR. Protein expression levels of **D**, phospho-vimentin and Twist-1, and E, BMPR-2 and PD-L1 in lung homogenates of SuHx rats (n=6). The data were generated from optical density measurements of individual bands normalized to β-actin and presented as fold change relative to Ctrl. Ctrl: healthy control; SuHx: SuHx for 8 weeks; SAHA: SuHx with SAHA 50 mg/kg/day. The data are presented as mean± SEM. n=5 to 6 for each group. *p<0.05, ** p<0.01, *** p<0.001, **** p<0.0001 compared with SuHx; ## p<0.01, ### p<0.001, #### p<0.0001 compared with Ctrl.

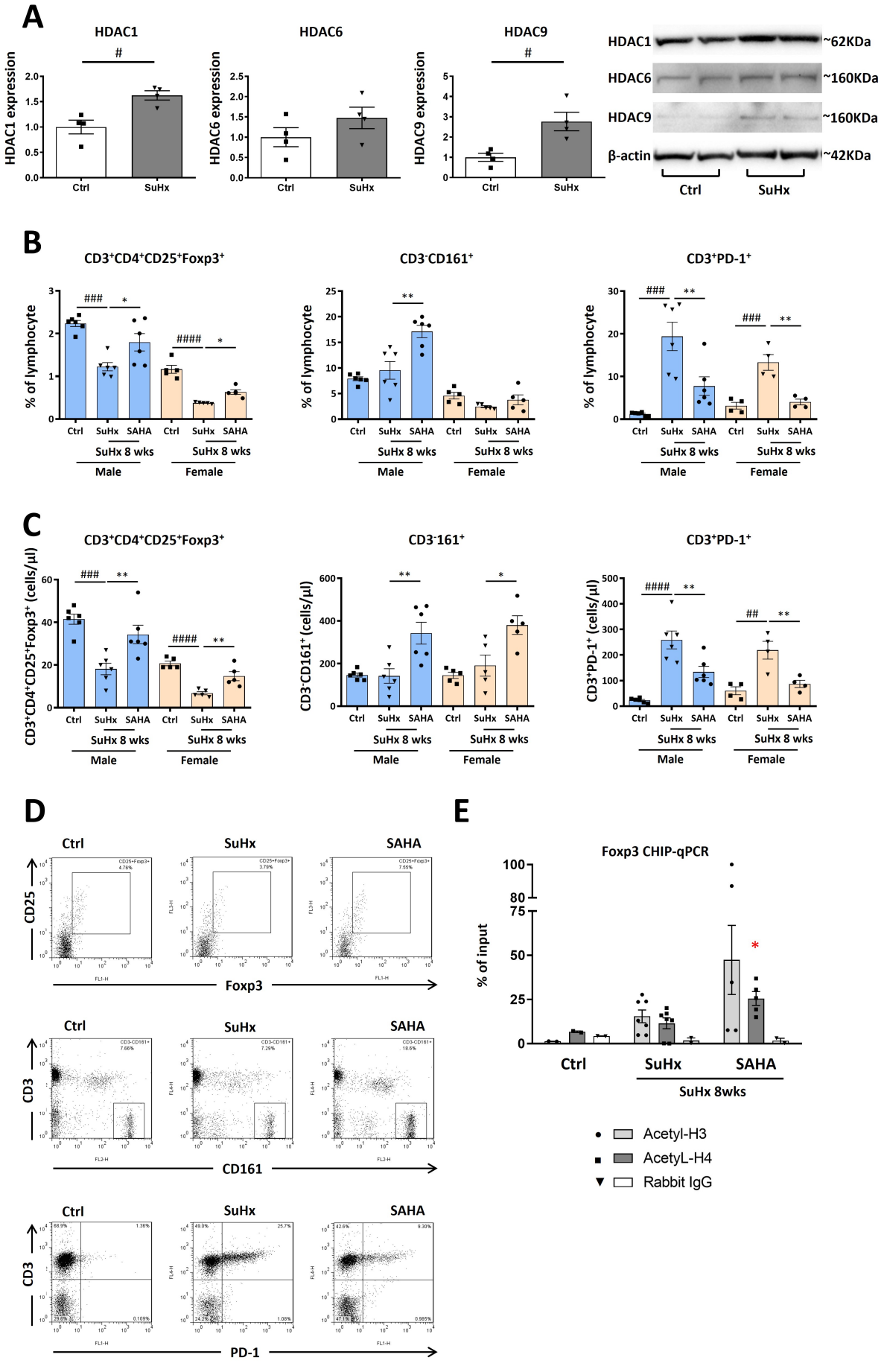
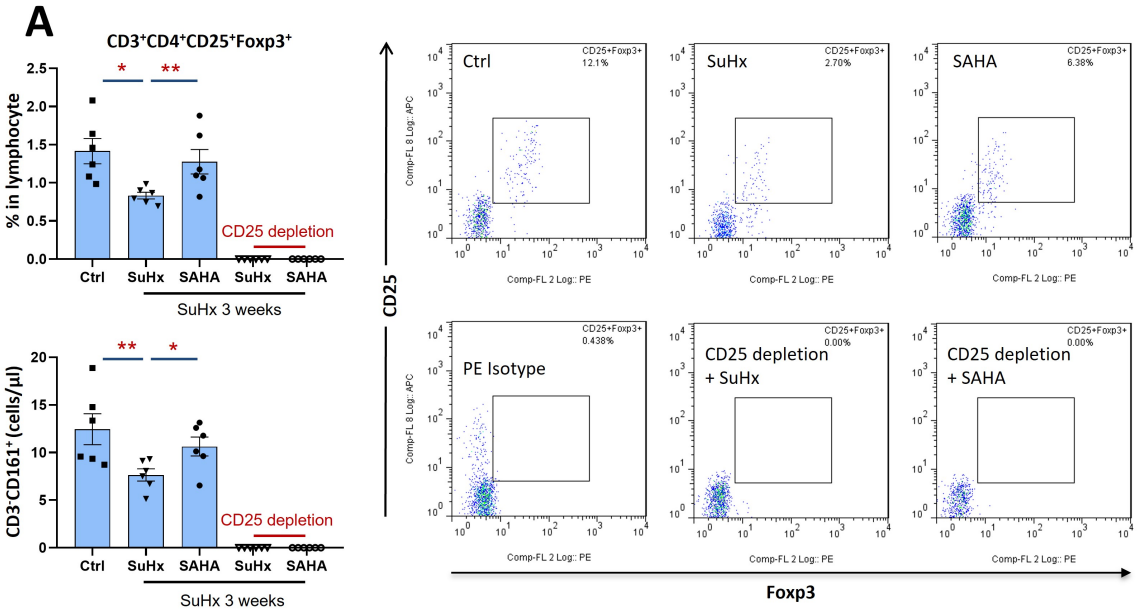
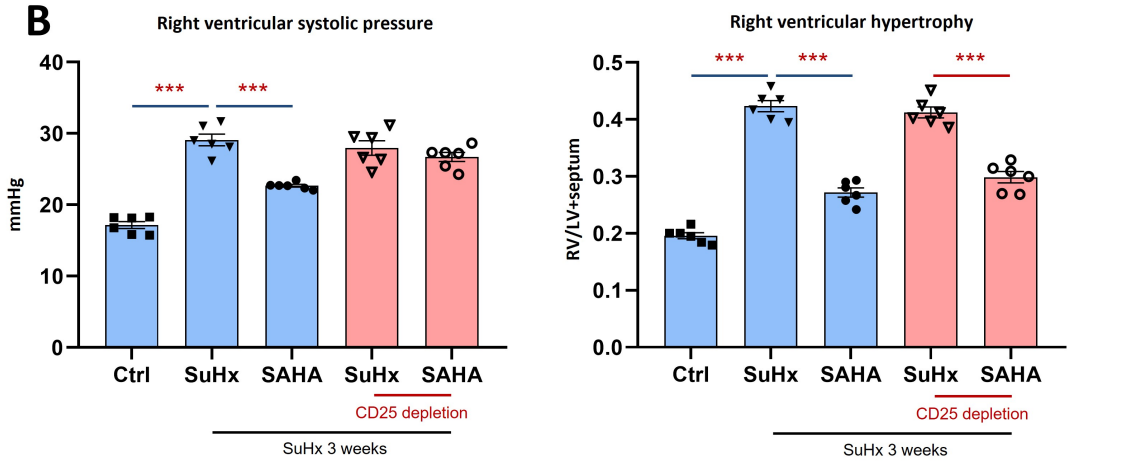

A
HDAC1
HDAC6
HDAC9
HDAC1 expression
HDAC6 expression
HDAC9 expression
Ctrl
SuHx
HDAC1 ~62KDa
HDAC6 ~160KDa
HDAC9 ~160KDa
β-actin ~42KDa
B
CD3+CD4+CD25+Foxp3+
CD3-CD161+
CD3+PD-1+
% of lymphocyte
SAHA
SuHx 8 wks
Male
Female
C
CD3+CD4+CD25+Foxp3+ (cells/μl)
CD3-CD161+ (cells/μl)
CD3+PD-1+ (cells/μl)
D
CD25
Foxp3
CD3
CD161
PD-1
E
Foxp3 CHIP-qPCR
% of input
SuHx 8wks
Acetyl-H3
AcetyL-H4
Rabbit IgG

Figure 6. SAHA increased circulating Treg and NK populations and decreased $CD3^+PD\text{-}1^+$ in SuHx rats in line with enrichment of acetylated histone bound to FOXP3 promoter. A, HDAC1, HDAC6 and HDAC9 expression levels in PBMCs from SuHx rats. The data were generated from optical density measurements of individual bands normalized to β-actin and presented as fold change relative to Ctrl. n=4. **B**, FACS analysis gated on lymphocyte population and the quantification of Treg ($CD3^+CD4^+CD25^+Foxp3^+$), NK ($CD3^-CD161^+$) cells and PD-1^+ T cells as the percentages of total lymphocytes and **C**, actual cell counts of peripheral $CD3^+CD4^+CD25^+Foxp3^+$, $CD3^-CD161^+$ and PD-1^+ T cells. Blue columns represent male rats (n=6); pink columns represent female rats (n=5).**D**, Representative dot plots of FACS analysis. **E**, ChIP pull-down of anti-acetylated H3/H4-associated chromatin, followed by qPCR for FOXP3 promoter. The data were quantified as the percentage of the input levels. Ctrl: healthy control; SuHx: SuHx for 8 weeks; SAHA: SuHx with SAHA 50 mg/kg/day. The data are presented as mean± SEM. n=6 for each group. * $p<0.05$, ** $p<0.01$ compared with SuHx; # $p<0.05$, ### $p<0.001$, #### $p<0.0001$ compared with Ctrl.


A
CD3+CD4+CD25+Foxp3+
% in lymphocyte
CD25 depletion
Ctrl
SuHx
SAHA
SuHx
SAHA
SuHx 3 weeks
CD3-CD161+ (cells/µl)
CD25 depletion
SuHx 3 weeks
CD25
Foxp3
Ctrl
SuHx
SAHA
PE Isotype
CD25 depletion + SuHx
CD25 depletion + SAHA
Comp-FL 2 Log:: PE
Comp-FL 8 Log:: APC


B
Right ventricular systolic pressure
mmHg
Right ventricular hypertrophy
RV/LV+septum
Ctrl
SuHx
SAHA
SuHx
SAHA
CD25 depletion
SuHx 3 weeks

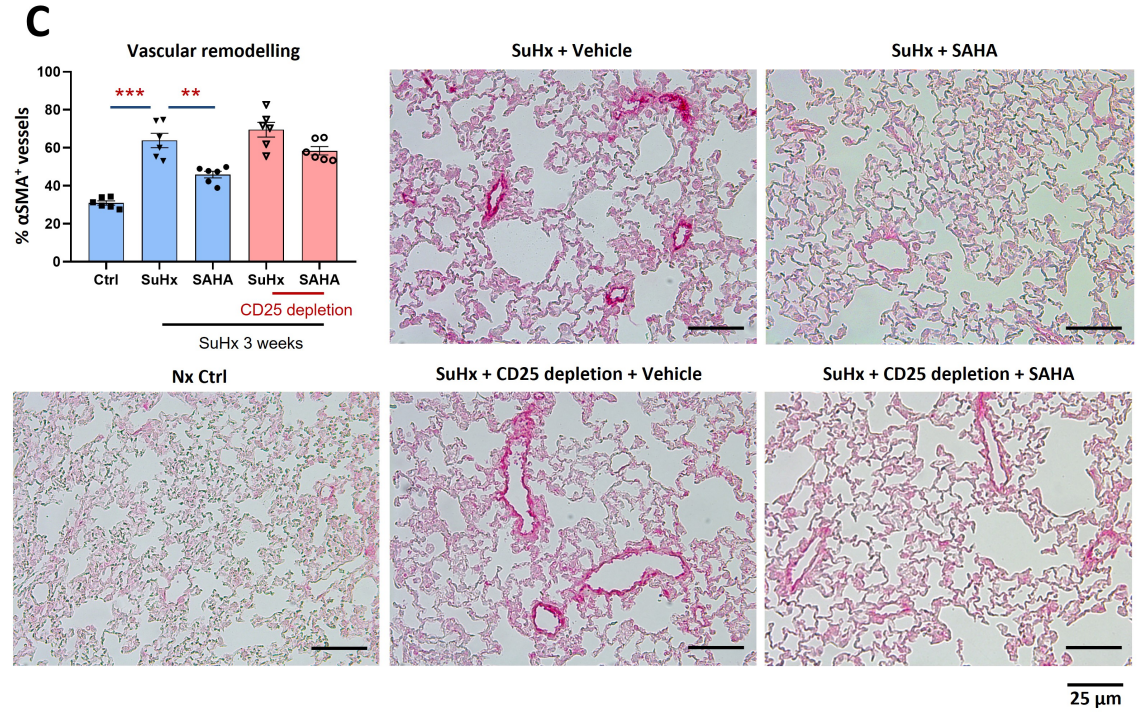
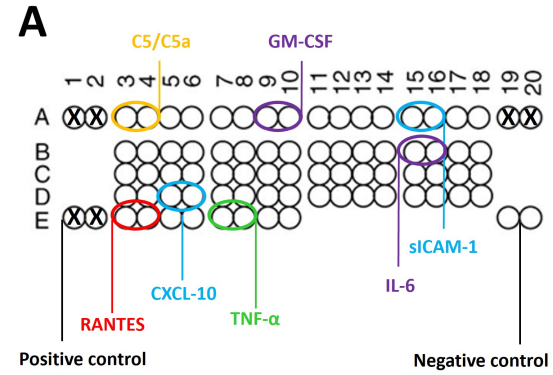
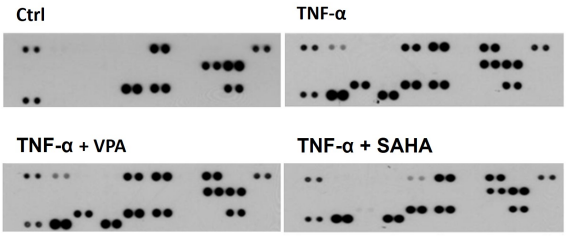
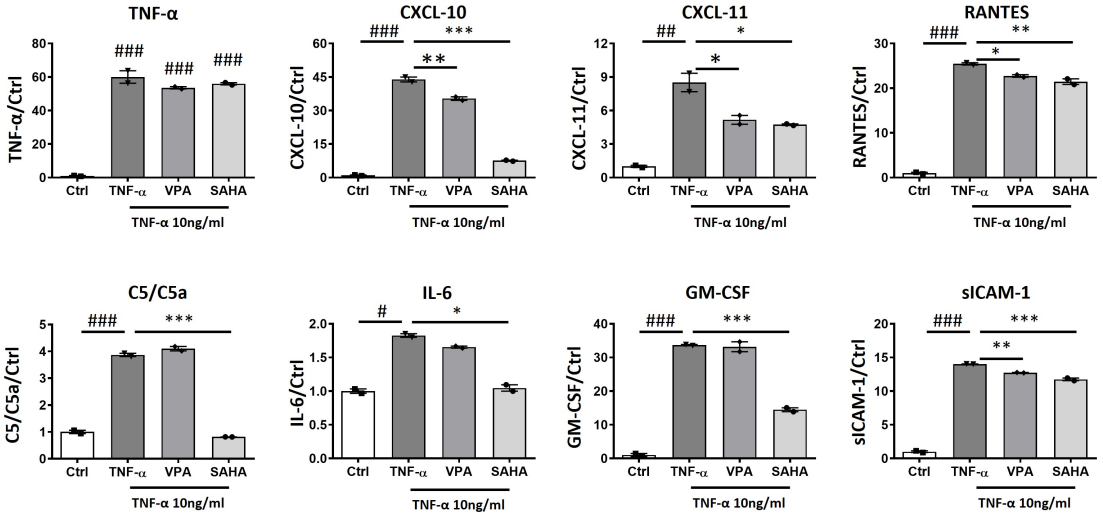

C
Vascular remodelling
% αSMA+ vessels
Ctrl
SuHx
SAHA
SuHx
SAHA
CD25 depletion
SuHx 3 weeks
SuHx + Vehicle
SuHx + SAHA
Nx Ctrl
SuHx + CD25 depletion + Vehicle
SuHx + CD25 depletion + SAHA
25 µm

Figure 7. The therapeutic effects of SAHA on SuHx-induced pulmonary hypertension in mice were neutralised by Treg depletion using anti-CD25 antibodies. A, The percentages in total lymphocytes and actual cell counts of circulating Treg ($CD3^+CD4^+CD25^+Foxp3^+$) cells in SuHx mice. **B**, Right ventricular systolic pressure, right ventricular hypertrophy quantified by RV/LV+septum ratio. **C**, the percentage of α smooth muscle actin (αSMA) positive muscularised vessels (diameter<50μm) and representative images of lung sections. Ctrl. Ctrl: healthy control; SuHx: SuHx for 8 weeks; SAHA: SuHx with SAHA 100 mg/kg/day. The data are presented as mean± SEM. n=6 for each group. *p<0.05, ** p<0.01, *** p<0.001, *** p<0.0001.



Coordinate	Target	Coordinate	Target	Coordinate	Target
A1, A2	Positive control	B9, B10	IL-2	D3, D4	IL-32[α]
A3, A4	C5/C5a	B11, B12	IL-4	D5, D6	CXCL-10
A5, A6	CD40 ligand	B13, B14	IL-5	D7, D8	CXCL-11
A7, A8	G-CSF	B15, B16	IL-6	D9, D10	MCP-1
A9, A10	GM-CSF	B17, B18	IL-8	D11, D12	MIF
A11, A12	CXCL1	C3, C4	IL-10	D13, D14	MIP-1α
A13, A14	CCL1	C5, C5	IL-12 p70	D15, D16	MIP-1β
A15, A16	sICAM-1	C7, C8	IL-13	D17, D18	Serpin E1
A17, A18	IFN-γ	C9, C10	IL-16	E1, E2	Positive control
A19, A20	Positive control	C11, C12	IL-17	E3, E4	RANTES
B3, B4	IL-1α	C13, C14	IL-17E	E5, E6	SDF-1
B5, B6	IL-1β	C15, C16	IL-23	E7, E8	TNF-α
B7, B8	IL-1ra	C17, C18	IL-27	E9, E10	sTREM-1
				E19, E20	Negative control





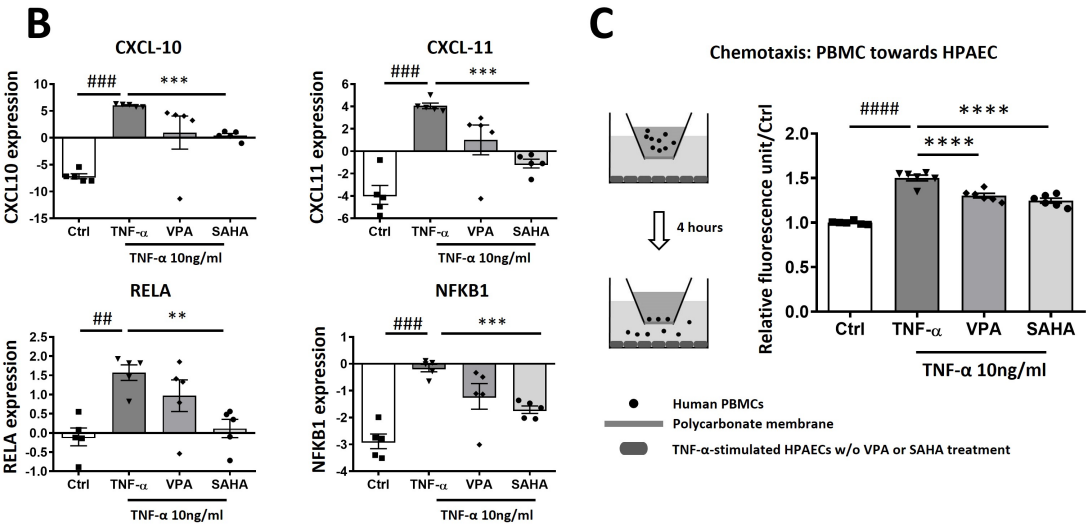


Figure 8. SAHA and VPA inhibited the release of inflammatory factors from TNF-α-stimulated HPAECs and the chemotaxis of leukocytes. A. Quantification of cytokine release from TNF-α-stimulated HPAECs in response to VPA (2 mmole/L) or SAHA (10 μmol/L) treatment detected by Panel-A cytokine array. The data were generated from optical density measurements of individual dots and normalized to positive control on each membrane. **B**. mRNA expression by RT-PCR: CXCL10, CXCL11, RELA and NFKB1. The relative expression of genes was presented as delta Ct values normalized to HPRT. **C**. Quantification of human PBMCs chemotaxis towards TNF-α-stimulated HPAECs w/o VPA or SAHA treatment. The data were calculated as fluorescence units relative to Ctrl. Ctrl: control without stimulation; TNF-α: TNF-α 10 ng/ml for 16 hours; VPA: TNF-α with VPA 2 mmole/L, and SAHA: TNF-α with SAHA 10 μmol/L. The data are presented as mean ± SEM. Experiments were performed in three independent biological replicates (n=3). * $p<0.05$, ** $p<0.01$, *** $p<0.001$ compared with TNF-α; # $p<0.05$, ## $p<0.01$, ### $p<0.001$ compared with Ctrl. TNF-α, tumor necrosis factor alpha; CXCL-10, chemokine (C-X-C motif) ligand 10; CXCL-11, chemokine (C-X-C motif) ligand 11; RANTES, regulated on activation, normal T cell expressed and secreted; C5/C5a, complement component 5/5a; IL-6, interleukin 6; GM-CSF, granulocyte-macrophage colony-stimulating factor; sICAM-1, soluble intercellular adhesion molecule 1; RELA, RELA proto-oncogene, NK-κB subunit; NFKB1, nuclear factor kappa B subunit1.

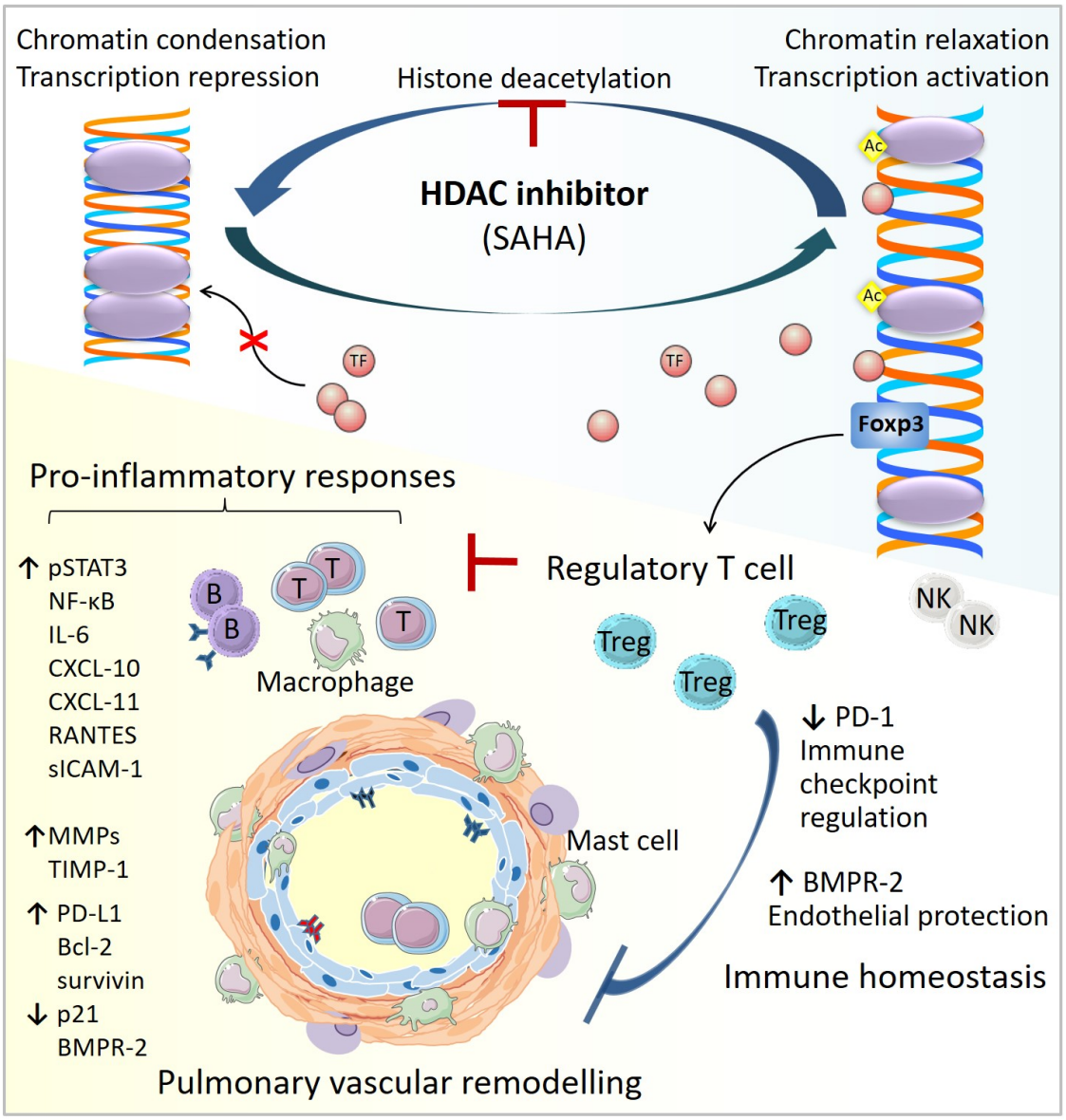


Figure 9. Proposed model of epigenetic mechanism by HDAC inhibition (SAHA, Vorinostat) in modulating Treg function and restoring immune homeostasis in PAH. Increased HDAC activity in the immune cells of PAH patients interferes with acetylation-dependent chromatin structures, leading to transcription repression. This is implicated in perivascular inflammatory cell infiltration, elevated extracellular matrix enzymatic activities, cytokine release and hyper-proliferation of vascular cells, contributing to the development and progression of PAH. HDAC inhibitor SAHA relaxes the chromatin structures, allowing more access of transcription factor binding to DNA and activating a cluster of epigenetic-sensitive gene expression involved in the immune-vascular crosstalk. Importantly, SAHA treatment induces FOXP3 expression and promotes Treg generation and function, restoring immune homeostasis and reversing pulmonary vascular remodeling. pSTAT3, phospho-signal transducer and activator of transcription 3; NF-κB, nuclear factor kappa B; IL-6, interleukin 6; CXCL-10, chemokine

(C-X-C motif) ligand 10; CXCL-11, chemokine (C-X-C motif) ligand 11; RANTES, regulated on activation, normal T cell expressed and secreted; sICAM-1, soluble intercellular adhesion molecule 1; MMPs, matrix metalloproteinases; TIMP-1, tissue inhibitor of metalloproteinase-1; PD-L1, programmed death-ligand 1; BMPR-2, bone morphogenetic protein receptor type 2; PD-1, programmed death-1; NK, natural killer cell.

Reference

1. Humbert M, Guignabert C, Bonnet S, Dorfmuller P, Klinger JR, Nicolls MR, *et al.* Pathology and pathobiology of pulmonary hypertension: state of the art and research perspectives. *Eur Respir J* 2019;53:1801887.
2. Huertas A, Perros F, Tu L, Cohen-Kaminsky S, Montani D, Dorfmuller P, *et al.* Immune dysregulation and endothelial dysfunction in pulmonary arterial hypertension: a complex interplay. *Circulation* 2014;129:1332–1340.
3. Jandl K, Marsh LM, Mutgan AC, Crnkovic S, Valzano F, Zabini D, *et al.* Impairment of the NKT–STAT1–CXCL9 Axis Contributes to Vessel Fibrosis in Pulmonary Hypertension Caused by Lung Fibrosis. *Am J Respir Crit Care Med* 2022;206:981–998.
4. Jones RJ, De Bie E, Groves E, Zalewska KI, Swietlik EM, Treacy CM, *et al.* Autoimmunity Is a Significant Feature of Idiopathic Pulmonary Arterial Hypertension. *Am J Respir Crit Care Med* 2022;206:81–93.
5. Huertas A, Tu L, Gambaryan N, Girerd B, Perros F, Montani D, *et al.* Leptin and regulatory T-lymphocytes in idiopathic pulmonary arterial hypertension. *Eur Respir J* 2012;40:895–904.
6. Huertas A, Phan C, Bordenave J, Tu L, Thuillet R, Le Hiress M, *et al.* Regulatory T Cell Dysfunction in Idiopathic, Heritable and Connective Tissue-Associated Pulmonary Arterial Hypertension. *Chest* 2016;149:1482–1493.
7. Taraseviciene-Stewart L, Nicolls MR, Kraskauskas D, Scerbavicius R, Burns N, Cool C, *et al.* Absence of T cells confers increased pulmonary arterial hypertension and vascular remodeling. *Am J Respir Crit Care Med* 2007;175:1280–1289.
8. Tamosiuniene R, Tian W, Dhillon G, Wang L, Sung YK, Gera L, *et al.* Regulatory T cells limit vascular endothelial injury and prevent pulmonary hypertension. *Circ Res* 2011;109:867–879.
9. C. Mickael LS R. Kumar B. Kassa M.H. Lee C. Abbott T.M. Bull K.R. Stenmark R.M. Tuder B.B. Graham. SG. Cd4+ T Cells Subsets Are Decreased in Peripheral Blood Mononuclear Cells (PBMCs) of Idiopathic Pulmonary Arterial Hypertension (IPAH) Patients Compared to Healthy Controls [abstract]. *Am J Respir Crit Care Med 2020;201:A3829*
10. Sakaguchi S, Yamaguchi T, Nomura T, Ono M. Regulatory T cells and immune tolerance. *Cell* 2008;133:775–787.
11. Placek K, Schultze JL, Aschenbrenner AC. Epigenetic reprogramming of immune cells in injury, repair, and resolution. *J Clin Invest* 2019;129:2994–3005.
12. Mazzone R, Zwergel C, Artico M, Taurone S, Ralli M, Greco A, *et al.* The emerging role of epigenetics in human autoimmune disorders. *Clin Epigenetics* 2019;11:34.

13. West AC, Johnstone RW. New and emerging HDAC inhibitors for cancer treatment. *J Clin Invest* 2014;124:30–39.
14. Zhao L, Chen CN, Hajji N, Oliver E, Cotroneo E, Wharton J, *et al.* Histone deacetylation inhibition in pulmonary hypertension: therapeutic potential of valproic acid and suberoylanilide hydroxamic acid. *Circulation* 2012;126:455–467.
15. Tao R, de Zoeten EF, Ozkaynak E, Chen C, Wang L, Porrett PM, *et al.* Deacetylase inhibition promotes the generation and function of regulatory T cells. *Nat Med* 2007;13:1299–1307.
16. Galie N, Humbert M, Vachiery JL, Gibbs S, Lang I, Torbicki A, *et al.* 2015 ESC/ERS Guidelines for the diagnosis and treatment of pulmonary hypertension: The Joint Task Force for the Diagnosis and Treatment of Pulmonary Hypertension of the European Society of Cardiology (ESC) and the European Respiratory Society (ERS): Endorsed by: Association for European Paediatric and Congenital Cardiology (AEPC), International Society for Heart and Lung Transplantation (ISHLT). *Eur Respir J* 2015;46:903–975.
17. Lucas JL, Mirshahpanah P, Haas-Stapleton E, Asadullah K, Zollner TM, Numerof RP. Induction of Foxp3+ regulatory T cells with histone deacetylase inhibitors. *Cell Immunol* 2009;257:97–104.
18. Zhao L, Chen CN, Hajji N, Oliver E, Cotroneo E, Wharton J, *et al.* Histone deacetylation inhibition in pulmonary hypertension: therapeutic potential of valproic acid and suberoylanilide hydroxamic acid. *Circulation* 2012;126:455–467.
19. Rhodes CJ, Wharton J, Ghataorhe P, Watson G, Girerd B, Howard LS, *et al.* Plasma proteome analysis in patients with pulmonary arterial hypertension: an observational cohort study. *Lancet Respir Med* 2017;5:717–726.
20. Darvin P, Toor SM, Sasidharan Nair V, Elkord E. Immune checkpoint inhibitors: recent progress and potential biomarkers. *Exp Mol Med* 2018;50:165.
21. Nijhuis L, Peeters JGC, Vastert SJ, van Loosdregt J. Restoring T Cell Tolerance, Exploring the Potential of Histone Deacetylase Inhibitors for the Treatment of Juvenile Idiopathic Arthritis. *Front Immunol* 2019;10:151.
22. Meloche J, Potus F, Vaillancourt M, Bourgeois A, Johnson I, Deschamps L, *et al.* Bromodomain-Containing Protein 4: The Epigenetic Origin of Pulmonary Arterial Hypertension. *Circ Res* 2015;117:525–535.
23. Vogel I, Kasran A, Cremer J, Kim YJ, Boon L, Van Gool SW, *et al.* CD28/CTLA-4/B7 costimulatory pathway blockade affects regulatory T-cell function in autoimmunity. *Eur J Immunol* 2015;45:1832–1841.
24. Hong KH, Lee YJ, Lee E, Park SO, Han C, Beppu H, *et al.* Genetic ablation of the BMPR2 gene in pulmonary endothelium is sufficient to predispose to pulmonary arterial hypertension. *Circulation* 2008;118:722–730.

25. Chelladurai P, Seeger W, Pullamsetti SS. Matrix metalloproteinases and their inhibitors in pulmonary hypertension. *Eur Respir J* 2012;40:766–782.
26. Travers JG, Wennersten SA, Pena B, Bagchi RA, Smith HE, Hirsch RA, *et al.* HDAC Inhibition Reverses Preexisting Diastolic Dysfunction and Blocks Covert Extracellular Matrix Remodeling. *Circulation* 2021;143:1874–1890.
27. Ranchoux B, Antigny F, Rucker-Martin C, Hautefort A, Pechoux C, Bogaard HJ, *et al.* Endothelial-to-mesenchymal transition in pulmonary hypertension. *Circulation* 2015;131:1006–1018.
28. Sofer A, Lee S, Papangeli I, Adachi T, Hwangbo C, Comhair S, *et al.* Therapeutic Engagement of the Histone Deacetylase IIA-Myocyte Enhancer Factor 2 Axis Improves Experimental Pulmonary Hypertension. *Am J Respir Crit Care Med* 2018;198:1345–1348.
29. Cavasin MA, Demos-Davies K, Horn TR, Walker LA, Lemon DD, Birdsey N, *et al.* Selective class I histone deacetylase inhibition suppresses hypoxia-induced cardiopulmonary remodeling through an antiproliferative mechanism. *Circ Res* 2012;110:739–748.
30. Rafikov R, Rischard F, Vasilyev M, Varghese M V, Yuan JX, Desai AA, *et al.* Cytokine profiling in pulmonary arterial hypertension: the role of redox homeostasis and sex. *Transl Res* 2022;247:1–18.
31. Chelladurai P, Kuenne C, Bourgeois A, Gunther S, Valasarajan C, Cherian A V, *et al.* Epigenetic reactivation of transcriptional programs orchestrating fetal lung development in human pulmonary hypertension. *Sci Transl Med* 2022;14:eabe5407.
32. Potus F, Pauciulo MW, Cook EK, Zhu N, Hsieh A, Welch CL, *et al.* Novel Mutations and Decreased Expression of the Epigenetic Regulator TET2 in Pulmonary Arterial Hypertension. *Circulation* 2020;141:1986–2000.
33. Wing JB, Tanaka A, Sakaguchi S. Human FOXP3(+) Regulatory T Cell Heterogeneity and Function in Autoimmunity and Cancer. *Immunity* 2019;50:302–316.
34. Zhu R, Xie X, Wang N, Chen L, Hong Y. The T helper type 17/regulatory T cell imbalance was associated with Ras-GTPase overexpression in patients with pulmonary hypertension associated with chronic obstructive pulmonary disease. *Immunology* 2019;157:304–311.
35. Liu Y, Shi JZ, Jiang R, Liu SF, He YY, van der Vorst EPC, *et al.* Regulatory T Cell-Related Gene Indicators in Pulmonary Hypertension. *Front Pharmacol*, 2022/06/18. 2022;13:908783.
36. Austin ED, Rock MT, Mosse CA, Vnencak-Jones CL, Yoder SM, Robbins IM, *et al.* T lymphocyte subset abnormalities in the blood and lung in pulmonary arterial hypertension. *Respir Med* 2010;104:454–462.

37. Ulrich S, Nicolls MR, Taraseviciene L, Speich R, Voelkel N. Increased regulatory and decreased CD8+ cytotoxic T cells in the blood of patients with idiopathic pulmonary arterial hypertension. *Respiration* 2008;75:272–280.
38. Jasiewicz M, Moniuszko M, Pawlak D, Knapp M, Rusak M, Kazimierczyk R, *et al.* Activity of the kynurenine pathway and its interplay with immunity in patients with pulmonary arterial hypertension. *Heart* 2016;102:230–237.
39. Sada Y, Dohi Y, Uga S, Higashi A, Kinoshita H, Kihara Y. Non-suppressive regulatory T cell subset expansion in pulmonary arterial hypertension. *Heart Vessels* 2016;31:1319–1326.
40. Savai R, Pullamsetti SS, Kolbe J, Bieniek E, Voswinckel R, Fink L, *et al.* Immune and inflammatory cell involvement in the pathology of idiopathic pulmonary arterial hypertension. *Am J Respir Crit Care Med* 2012;186:897–908.
41. Qiu H, He Y, Ouyang F, Jiang P, Guo S, Guo Y. The Role of Regulatory T Cells in Pulmonary Arterial Hypertension. *J Am Heart Assoc* 2019;8:e014201.
42. Tamosiuniene R, Manouvakhova O, Mesange P, Saito T, Qian J, Sanyal M, *et al.* Dominant Role for Regulatory T Cells in Protecting Females Against Pulmonary Hypertension. *Circ Res* 2018;122:1689–1702.
43. Bolden JE, Shi W, Jankowski K, Kan CY, Cluse L, Martin BP, *et al.* HDAC inhibitors induce tumor-cell-selective pro-apoptotic transcriptional responses. *Cell Death Dis* 2013;4:e519.
44. Mantel PY, Ouaked N, Ruckert B, Karagiannidis C, Welz R, Blaser K, *et al.* Molecular mechanisms underlying FOXP3 induction in human T cells. *J Immunol* 2006;176:3593–3602.
45. Cui J, Xu H, Yu J, Li Y, Chen Z, Zou Y, *et al.* IL-4 inhibits regulatory T cells differentiation by HDAC9-mediated epigenetic regulation. *Cell Death & Disease 2021 12:6* 2021;12:1–11.
46. de Zoeten EF, Wang L, Sai H, Dillmann WH, Hancock WW. Inhibition of HDAC9 increases T regulatory cell function and prevents colitis in mice. *Gastroenterology* 2010;138:583–594.
47. Beier UH, Wang L, Han R, Akimova T, Liu Y, Hancock WW. Histone deacetylases 6 and 9 and sirtuin-1 control Foxp3+ regulatory T cell function through shared and isoform-specific mechanisms. *Sci Signal* 2012;5:ra45.
48. Nie J, Li YY, Zheng SG, Tsun A, Li B. FOXP3+ Treg cells and gender bias in autoimmune diseases. *Front Immunol* 2015;6:493.
49. Pilat N, Sprent J. Treg Therapies Revisited: Tolerance Beyond Deletion. *Front Immunol* 2020;11:622810.

50. Ormiston ML, Chang C, Long LL, Soon E, Jones D, Machado R, *et al.* Impaired natural killer cell phenotype and function in idiopathic and heritable pulmonary arterial hypertension. *Circulation* 2012;126:1099–1109.
51. George PM, Oliver E, Dorfmuller P, Dubois OD, Reed DM, Kirkby NS, *et al.* Evidence for the involvement of type I interferon in pulmonary arterial hypertension. *Circ Res* 2014;114:677–688.
52. Tomaszewski M, Grywalska E, Tomaszewski A, Blaszczak P, Kurzyna M, Rolinski J, *et al.* Overexpression of PD-1 on Peripheral Blood Lymphocytes in Patients with Idiopathic Pulmonary Arterial Hypertension and Its Association with High Viral Loads of Epstein-Barr Virus and Poor Clinical Parameters. *J Clin Med* 2020;9:1966.
53. Sambucci M, Gargano F, De Rosa V, De Bardi M, Picozza M, Placido R, *et al.* FoxP3 isoforms and PD-1 expression by T regulatory cells in multiple sclerosis. *Sci Rep* 2018;8:3674.
54. Liu Y, Pang Y, Hu Z, Wu M, Wang C, Feng Z, *et al.* Thymosin alpha 1 (Talpha1) reduces the mortality of severe COVID-19 by restoration of lymphocytopenia and reversion of exhausted T cells. *Clin Infect Dis* 2020;71:2150-2157.
55. Caldrer S, Mazzi C, Bernardi M, Prato M, Ronzoni N, Rodari P, *et al.* Regulatory T Cells as Predictors of Clinical Course in Hospitalised COVID-19 Patients. *Front Immunol* 2021;12:789735.
56. Celada LJ, Kropski JA, Herazo-Maya JD, Luo W, Creecy A, Abad AT, *et al.* PD-1 up-regulation on CD4(+) T cells promotes pulmonary fibrosis through STAT3-mediated IL-17A and TGF-beta1 production. *Sci Transl Med*, 2018/09/28. 2018;10:eaar8356.
57. Kronborg-White S, Madsen LB, Bendstrup E, Poletti V. PD-L1 Expression in Patients with Idiopathic Pulmonary Fibrosis. *J Clin Med* 2021;10:5562.
58. Weyand CM, Rg J, Goronzy J. T cell aging in hypertension. *Cardiovasc Res* 2021;117:21–23.
59. Mylvaganam R, Avery R, Goldberg I, Makowski C, Kalhan R, Villaflor V, *et al.* Adverse effects of immune checkpoint inhibitor therapies on right ventricular function and pulmonary arterial dilatation. *Pulm Circ* 2021;11: 2045894021992236.
60. Boehm F, Martin M, Kesselring R, Schiechl G, Geissler EK, Schlitt H-J, *et al.* Deletion of Foxp3 + regulatory T cells in genetically targeted mice supports development of intestinal inflammation. 2012;12:97.